Summer 2021

Stable Isotope Analysis Reveals Differences in Domoic Acid Accumulation and Feeding Strategies of Key Vector Species in Central California

Sophie Brynn Bernstein

STABLE ISOTOPE ANALYSIS REVEALS DIFFERENCES IN DOMOIC ACID ACCUMULATION AND FEEDING STRATEGIES OF KEY SPECIES IN CENTRAL CALIFORNIA

A Thesis

Presented to the

Faculty of

Moss Landing Marine Laboratories

California State University Monterey Bay

In Partial Fulfillment

of the Requirements for the Degree

Master of Science

in

Marine Science

---

by

Sophie Brynn Bernstein

Summer 2021

CALIFORNIA STATE UNIVERSITY MONTEREY BAY

The Undersigned Faculty Committee Approves the

Thesis of Sophie Brynn Bernstein:

STABLE ISOTOPE ANALYSIS REVEALS DIFFERENCES IN DOMOIC ACID ACCUMULATION AND FEEDING STRATEGIES OF KEY SPECIES IN CENTRAL CALIFORNIA

DocuSigned by:
Scott Hamilton
FAE6F563920F4E8...

Scott Hamilton, Chair

Moss Landing Marine Laboratories

DocuSigned by:
Rocio Iliana Ruiz-Cooley
1223D67B66A349E...

Rocio Iliana Ruiz Cooley

Moss Landing Marine Laboratories & Centro de Investigación Científica y de Educación Superior de Ensenada

DocuSigned by:
Max Grand
206813748B5D466...

Maxime Grand

Moss Landing Marine Laboratories

Doug Smith 27 August 2021

Dean

Dean of Undergraduate and Graduate Studies

_____

Approval Date

DEDICATION

I dedicate this thesis to a select few individuals who supported my development as a scholar between elementary and graduate school. First, my parents, Jill and Robbie, for providing me with resources to flourish and building a network of advocates for me from a young age, and my siblings, Ben and Emma for setting high intellectual standards. Second, Ms. Braun, my Learning Resource Center teacher who I worked with 4x/week for 4-years in high school. She offered me with consistent praise for my work ethic and reminded me that I had the tools to succeed. Finally, I include Dr. Morgan Benowitz-Fredericks, the professor at Bucknell University whose course I took in Spring 2016. Her *Animal Behavior* class altered the trajectory of my career.

ABSTRACT

Stable isotope analysis reveals differences in domoic acid accumulation and feeding strategies of key vector species in central California

by

Sophie Brynn Bernstein

Masters of Marine Science in Marine Science

California State University Monterey Bay, 2021

Given the effects of harmful algal blooms (HABs) on human and wildlife health, understanding how domoic acid (DA) is accumulated and transferred through food webs is critical for recognizing the most affected marine communities and predicting ecosystem effects. This study combines stable isotopes of carbon ($\delta^{13}C$) and nitrogen ($\delta^{15}N$) from bulk muscle tissue with DA measurements from viscera to identify the foraging strategies of important DA vectors and predators in Monterey Bay, CA. Tissue samples were collected from 23 species across three habitats in the summer of 2018 and 2019 (time periods without prominent HABs), with a focus on California sea lions, as the primary predator affected by DA, their prey (anchovies, sardines, squid, krill, juvenile rockfish), and other key sentinel species (e.g., mussels). My results highlight ^{13}C enrichment in krill and elevated DA concentrations ([DA]; ppm) in anchovies collected inside Monterey Bay, indicating inshore-offshore differences in coastal productivity and DA accumulation. The narrow, overlapping isotopic niches between anchovies and sardines and striking differences in [DA], suggests these common prey species exhibit dietary specialization and resource partitioning, potentially based on prey size. In contrast, krill, market squid, and juvenile rockfish accumulated minimal DA during 2018/19 and thus have a lower capacity to serve as DA vectors during years of low HAB activity. Low [DA] in the livers of stranded sea lions along with their large isotopic niche may indicate that individuals have different diets or feed in isotopically distinct locations limiting the ability to use sea lions as sentinels for DA outbreaks in a specific geographic area. Collectively, my results show that DA was produced a few kilometers from the coastline and that anchovies were the most powerful DA vector in coastal-pelagic zones (potentially associated with their feeding specialization and high mobility), while mussels did not contain detectable DA in the years of sampling (despite their status as the key indicator of DA in coastal systems) and only reflect *in situ* DA, $\delta^{13}C$, and $\delta^{15}N$ values. In comparison, anchovy DA loads in this study consistently exceeded FDA regulatory limits for human consumption. The findings demonstrate the efficacy of combining multiple biogeochemical tracers to improve HAB monitoring efforts and identifying routes of DA transfer across habitats and trophic levels.

ACKNOWLEDGEMENTS

This research was supported by the California Sea Grant R/HCE-05 and was made possible by a larger team of collaborators. A sincere thank you to Dr. Iliana Ruiz-Cooley, Dr. Scott Hamilton and Dr. Maxime Grand, my advisors and thesis committee members, and Dr. Gitte McDonald. Specifically, to Iliana, who blindly accepted me as the student to work on her project and taught me that perseverance and grit is necessary in this field. I also thank Dr. Clarissa Anderson, Dr. Robin Dunkin, Dr. John Field and Dr. Raphe Kudela, the coauthors on the manuscript associated with this thesis research:

> Bernstein, S., R. I. Ruiz Cooley., R. Kudela., C. Anderson., R. Dunkin., J. Field., Stable isotope analysis reveals differences in domoic acid accumulation and feeding strategies of key vectors in a California hotspot for outbreaks. *Harmful Algae. In Review*

Each of these coauthors provided invaluable feedback and graciously shared their time and expertise. I entered graduate school with a pure love of learning and for the ocean, and with the help of these mentors, I developed the knowledge base I have long yearned for and am excited to pursue a career in science

Collaborators also include those who provided us with specimens. These include: the Southwest Fisheries Science Center who conducted the Rockfish Recruitment and Ecosystem Assessment surveys in 2018 and 2019, Dan Kamikawa (NOAA; NMFS) and Justin Cordova (Moss Landing Marine Laboratories; MLML) for collecting specimens on the West Coast Groundfish Bottom Trawl Surveys in 2018; Karolina Wirga and Amber Diluzio from the Marine Mammal Stranding Network at UCSC for providing marine mammal tissue samples; the Marine Operations team at MLML for assisting with collecting Dungeness crabs on the R/V *Sheila B* (sport permit 1066991024). I also thank those who supported with laboratory analyses: Sharon Hsu and Matthew Jew from MLML for dissecting and preparing specimens for laboratory analyses and Kendra Negrey at UCSC for helping coordinate toxin measurements.

Finally, I want to thank those who supported me personally over the last several years. This includes Kim, Nate, Chris, Connor, Booker and Natalie Ward who became my second family, and my local friends who encouraged me to balance adventure with academics.

TABLE OF CONTENTS

LIST OF FIGURES & TABLES

INTRODUCTION

Harmful Algal Blooms (HABs) are increasing in frequency, intensity, and geographic range, threatening open ocean and coastal ecosystems worldwide (Bates et al., 2018). In the California Current System (CCS), HABs have been documented nearly every year since 1998, concurrent with anthropogenic stressors that alter nutrient distributions and phytoplankton assemblages (Sun et al., 2011; Lewitus et al., 2012; Trainer et al., 2020). A majority of these HABs are associated with domoic acid (DA), a toxin produced by *Pseudo-nitzschia* spp*.,* including the prolific toxin-producers, *Pseudo-nitzschia multiseries* and *Pseudo-nitzschia australis* (Horner et al., 1997; Trainer et al., 2000). When ingested by humans, DA can cause the potentially fatal Amnesic Shellfish Poisoning (Bates et al., 1989). As a result, commercial and recreational shellfish and finfish fisheries, including Dungeness crab (*Metacarcinus magister*), anchovy (*Engraulis mordax*), and sardine (*Sardinops sagax*), are closely monitored to protect human health (Lewitus et al., 2012; Anderson et al., 2019). These fisheries are particularly susceptible to seasonal closures in response to DA outbreaks, often resulting in economic hardship for coastal communities (McCabe et al., 2016; Ritzman et al., 2018; Holland and Leonard, 2020). DA episodes are also responsible for mass morbidity and mortality of marine mammals and seabirds, thereby threatening ecosystem balance (Work et al., 1993; Scholin et al., 2000). Yet, detailed, comparative explanations on the role that foraging strategies play in explaining the capacity for a given species to serve as a DA vector have

not been provided, and, as a result, detecting the onset of a toxic event is often delayed. These topics are addressed in the current study.

The widespread ecosystem consequences of DA events call for abundant monitoring and forecasting initiatives, which are limited in capacity because of the challenges of acquiring data from non-coastal regions. Phytoplankton composition and water quality are measured weekly at nine coastal sites in California (Anderson et al., 2019). DA concentrations from mussels are also measured routinely at some sites. At the Santa Cruz Municipal Wharf (SCMW), specifically, DA concentrations in mussels align well with particulate DA (pDA) concentrations from phytoplankton in the water, making mussels reliable indicators of DA accumulation in primary consumers and toxin presence along the coastline (Lane et al., 2009; Anderson et al., 2016); however, these routine efforts only detect HABs within ~4km from the shoreline (Kudela et al., 2012; Frolov et al., 2013). The precise locations of bloom initiation and DA production are not clearly identified because the oceanographic conditions favoring such blooms are spatially and temporally variable, and not all *Pseudo-nitzschia* spp. produce toxins (Lelong et al., 2012; Bates et al., 2018). The species composition of toxin-producing phytoplankton communities determines the level of DA production, and is highly influenced by temperature, micro- and macro-nutrient concentrations, among other factors, which vary in space and time (Trainer et al., 2020). This was evident during 2015, when *Pseudo-nitzschia* blooms were initiated by anomalously warm ocean conditions and biophysical changes. In Monterey Bay, California, blooms became toxic after upwelling removed warm waters and shifted nutrient ratios within organisms (Ryan et al., 2017) while DA production along coastal Oregon and Washington was driven mainly by spring storms

delivering blooms from offshore waters (McCabe et al., 2016). Phytoplankton communities can also shift rapidly due to wind forcing, the influx of different water masses, and stratification of the water column (Ryan et al., 2011, 2014). The spatial and temporal complexity surrounding DA production makes it difficult to predict the primary routes of DA trophic transfer.

The routes of DA transfer and exposure to consumers are difficult to determine given that being an active DA vector likely depends on the intensity of the toxic-forming HAB event, the length of time spent foraging in a toxic bloom, and the foraging strategy of the consumer. An active DA vector may be defined operationally as one whose viscera content exceeds federal regulatory limits of 20 ppm (California Ocean Science Trust, 2016) and is capable of transferring DA to higher trophic levels. It is also challenging to determine the effect of DA on the ecosystem and predict the fisheries resources impacted by toxic events because DA can enter the food web through both pelagic and benthic pathways (Vigilant and Silver, 2007). The most recognized mechanism of DA transfer to high trophic predators in pelagic regions is through primary and secondary consumers (e.g. krill, anchovies, sardines, juvenile fishes) that directly consume toxic algal cells and accumulate DA in their digestive system (Scholin et al., 2000; Bargu et al., 2002; Lefebvre et al., 2002b). Most of these taxa are important forage species in the California Current (Szoboszlai et al., 2015) and have been deemed the causal agent of acute and chronic DA toxicosis in California sea lions (*Zalophus californianus*), an abundant coastal marine predator often considered a sentinel for offshore DA events (Lefebvre et al., 1999; Gulland et al., 2002; Bargu et al., 2012). In contrast, Dungeness crabs are exposed to DA through benthic pathways, potentially through DA preserved and

resuspended in sediments or by consuming various filter-feeding invertebrates (Lefebvre and Robertson, 2010). The ability to predict where and when prey taxa and predators ingest DA is not fully understood, in part due to their high mobility and broad foraging areas.

Efforts to identify DA vectors and the cause of sea lion mortality frequently focus on analyzing viscera through stomach content analysis (SCA), and urine and fecal analysis (FA). These methods provide the most consistent data, especially because DA is rapidly excreted by top predators and their prey (Gulland, 2000; Lefebvre et al., 2002b). SCA and FA offer detailed information on recently ingested prey items, and were the primary methods used to link sea lion mortality to prey with high DA concentrations (Lefebvre et al., 1999; Scholin et al., 2000). Yet, such methods poorly detect items that are highly digested and do not provide information on what or where a consumer was eating over longer time frames (Hyslop, 1980). As a result, explanations for why certain taxa are critical DA vectors to higher trophic level consumers do not consider how DA varies spatially, nor do they consider how life history and foraging strategy contribute to toxin accumulation. A more comprehensive study of taxa that accumulate DA from different habitats is necessary for understanding how DA is dispersed and transferred through marine ecosystems, and ultimately, for improving HAB response efforts.

The objectives of this study were to identify key trophic pathways of DA transfer in the Monterey Bay food web and to determine the habitats and regions prone to DA accumulation during years without highly anomalous ocean conditions or major, known toxic blooms. This work incorporates a mixed method approach encompassing DA measurements and stable isotope analysis of carbon ($\delta^{13}C$) and nitrogen ($\delta^{15}N$) from

animal tissues. While there have been food web studies focusing on DA in Monterey Bay (e.g. Lefebvre et al., 2002a; Bargu et al., 2002, 2008), DA measurements and isotopes have not been integrated in the same study. The combined approach in this project allowed spatial variation in elemental cycling and DA accumulation in consumers to be identified and used isotopic niches to determine important trophic links and foraging strategies that influence toxin accumulation in DA vectors from different habitats.

Stable isotopes of carbon ($\delta^{13}C$) and nitrogen ($\delta^{15}N$) provide an integrated view of the diet and habitat use of consumers (Peterson and Fry, 1987; DeNiro and Epstein, 1978, 1981). The $\delta^{13}C$ from an organism reflects the source of carbon that primary producers use for photosynthesis (Smith and Epstein, 1971) and this metric can be used to differentiate between coastal and pelagic foragers in marine systems (Burton and Koch, 1999). Overall, higher $\delta^{13}C$ values are associated with productive regions, including coastal upwelling zones like that of the CCS (Rau et al., 1982; Goericke and Fry, 1994). The $\delta^{15}N$ values from primary producers also vary geographically based on a region's dominant N source and the degree of NO_3^- uptake by phytoplankton, relative to other sources of N (i.e., NH_4^+, NO_2^-) (Liu and Kaplan, 1989; Altabet et al., 1999). These $\delta^{13}C$ and $\delta^{15}N$ baseline values from primary producers and prey items are integrated throughout consumer diets, creating variation across marine ecosystems and habitats and allowing for nutrient and source information to be inferred (Ruiz-Cooley et al., 2012; Ruiz-Cooley and Gerrodette, 2012). The trophic position of an organism is also reflected by the relative values of $\delta^{13}C$ and $\delta^{15}N$, given the predictable stepwise enrichment between predator and their prey (3 to 4‰ for $\delta^{15}N$; 0.5 to 1‰ for $\delta^{13}C$) (DeNiro and Epstein, 1981; Minagawa and Wada, 1984; Post, 2002). The range of isotope values

expressed in a population determines the size of its 'isotopic niche,' providing ecological information on diet and nutrient sources, trophic position, and foraging strategies (Layman et al., 2007; Newsome et al., 2007; Flaherty and Ben-David, 2010).

By interpreting DA measurements from potential vectors with their isotopic niche and suggested feeding behavior, it is possible to identify species-specific foraging strategies and explain why certain consumers have a higher capacity to accumulate and transfer DA to top predators than others. I hypothesized that a species is more likely to accumulate and disperse toxins throughout the food web if they are primary consumers and have a narrow isotopic niche representing a subpopulation of dietary specialists and mobile habitat specialists (enabling dietary consumption over large geographic ranges). In contrast, species with broader isotopic niches, whose individuals are diet generalists, may be less likely to accumulate DA. Since C and N sources and cycling process vary spatially, I also expected to document heterogeneity in baseline isotope values and DA accumulation at a longitudinal level. Such spatial variation may reflect the inshore-offshore decoupling documented in previous studies and reveal regions where toxins accumulate in Monterey Bay, even during periods without massive coastwide blooms.

Methods

Study Site and Sample Collection

The Monterey Bay is a highly dynamic coastal upwelling region and an ideal ecosystem to assess the accumulation of DA in consumers because the phytoplankton assemblage is dominated by diatoms, including *Pseudo-nitzschia* spp. that form toxic HABs (Garrison, 1979; Horner et al., 1997; Smith et al., 2018). Such blooms are

supported by water and nutrient influx from several sources, including new nutrients from seasonal, spring upwelling and Ekman pumping, and regional water circulation patterns that retain water and nutrients in parts of Monterey Bay (Rosenfeld et al., 1994; Graham and Largier, 1997; Checkley and Barth, 2009). The Monterey Bay also receives nutrient inputs from estuaries and rivers, including the Elkhorn Slough, San Lorenzo River, and Pajaro River, all of which are susceptible to high nutrient loads from agricultural runoff (Lane et al., 2009; Lecher et al., 2015).

Efforts to collect specimens focused on 2018, a year characterized by less anomalous oceanographic conditions following the 2014-16 large marine heatwave. HAB conditions along the coast were returning to conditions closer to the recent long-term average. Despite localized DA events in HAB hotspots, there were no region-wide HABs nor fishery closures in Monterey Bay. The Pacific Decadal Oscillation and Oceanic El Niño Index were close to neutral conditions north of Point Conception in the CCS (Thompson et al., 2018; Harvey et al., 2019). Collections for DA and stable isotope analysis primarily targeted potential DA vectors, commercially important species, and California sea lions. Samples were collected over a range of depths and distance to shore gradients, covering coastal-pelagic, coastal-benthic, and deep-benthic habitats (Fig. 1). Potential DA vectors are defined as taxa capable of filter feeding or feeding on micronekton that contain DA, and include northern anchovy (*Engraulis mordax*), krill (*Euphausia pacifica* and *Thysanoessa spinifera*), pelagic juvenile rockfish (*Sebastes semicinctus, Sebastes jordani, Sebastes saxicola,* and *Sebastes goodei*), Pacific sardine (*Sardinops sagax*), market squid (*Doryteuthis opalescens*), and mussels (*Mytilus californianus*). These species cover four of the five primary functional forage taxa in the

CCS (Szoboszlai et al., 2015; Koehn et al., 2016). Additional samples of taxa that are not suspected DA vectors were opportunistically collected. These include algae and echinoderms from Moss Landing Harbor (MLH) (Fig. 1), and cephalopods, benthic fish, cartilaginous fish, echinoderms, and crustaceans from West Coast Groundfish Bottom Trawl Surveys (WCGBTS) (Appendix T1).

Table 1. Sample collections and estimated trophic position of the potential vectors and California sea lions: Station numbers 109-212 represent the original NOAA-SWFSC field station where specimens were collected (see Fig. 1). SCW: Santa Cruz Wharf. MLH: Moss Landing Harbor. Trophic position (TP) was estimated following Post (2002)'s equation. The mean C:N ratio and standard deviation (SD) is shown for all specimens of a given species analyzed. A full list of all species collected can be found in the appendix.

Species	Stations Collected	Total Sample Size	TP	Mean C:N (SD)
Anchovy	113-117; 119; 211; 110/212	69	3.08	3.74 (1.45)
Krill	113; 114; 116; 117; 119; 110/212	16	2.2	3.66 (0.19)
Juvenile Rockfish	109; 113-117; 119; 212	46	2.87	3.63 (0.17)
Sardine	113-114; 116; 211; 110/212	29	2.95	3.44 (0.25)
Market Squid	114; 115; 119; 110/212	28	2.93	3.47 (0.05)
Mussel	SCW; MLH	6	2.2	3.87 (0.17)
Sea Lion	Beaches within Monterey Bay	8	4.16	3.29 (0.19)
Dungeness Crab	C1,2	29	3.46	3.22 (0.07)

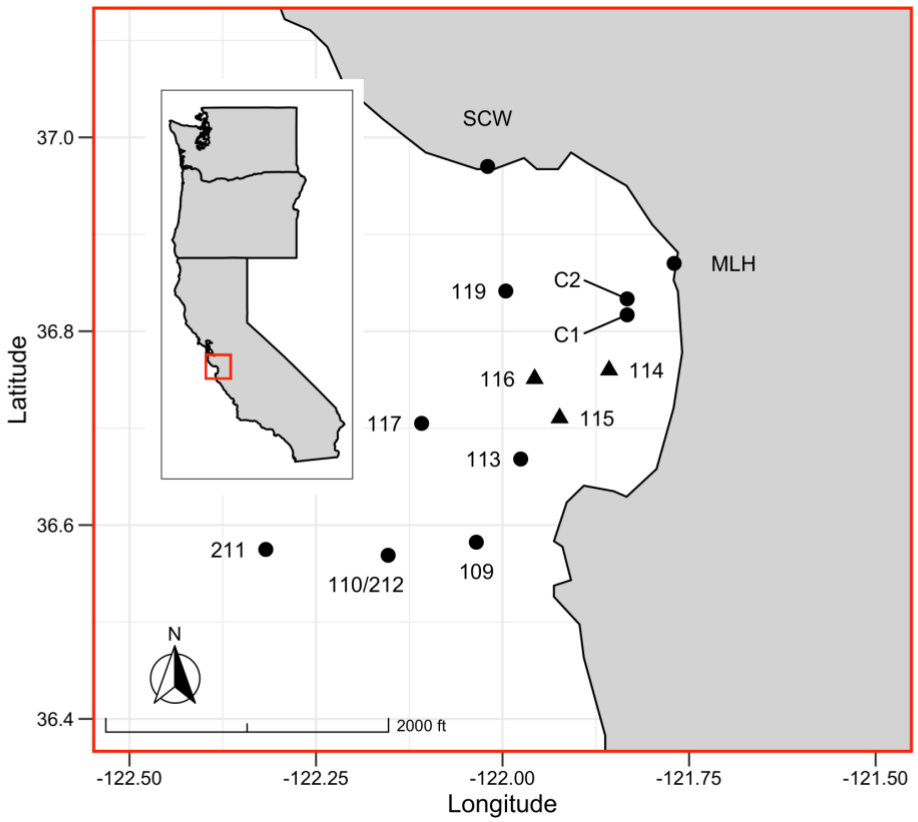

Figure 1. Sites of specimen collections from Monterey Bay in 2018. Moss Landing Harbor (MLH). Santa Cruz Wharf (SCW). NOAA sampling sites from RREAS (109-212). Dungeness Crab collection sites (C1, 2). Triangles are stations included in the site-control analysis. Inlet map is provided to show the geographical location of Monterey Bay along the U.S. West Coast. The San Lorenzo River passes through Santa Cruz, entering the northern part of the bay. The Elkhorn Slough and Pajaro River discharge nearby MLH.

All potential DA vectors, except for mussels, were collected on the Rockfish Recruitment and Ecosystem Assessment Survey (RREAS), conducted off of California in late spring of each year (Sakuma et al. 2016). Dates of sample collection ranged from May 14 to June 15, 2018. WCGBTS from 2018 accounted for a portion of the specimens analyzed (Appendix T1). Mussels were obtained onsite at the SCW and MLH (Fig. 1). Additional sardine and anchovy specimens were collected between May 5 and June 7, 2019 on the RREAS and were included to increase sample sizes and power of analysis

because only eight sardines were collected from 2018. Dungeness crabs from June 2019 were collected near Moss Landing (Fig. 1) on the R/V *Sheila B*, using recreational crab traps. They were included to incorporate isotope information from a commercially valuable fishery that is prone to extensive closures during HABs (Ritzman et al., 2018; Holland and Leonard, 2020).

Sea lion muscle and liver tissues were provided by the Marine Mammal Stranding Network at Moss Landing Marine Laboratories (MLML) and UC Santa Cruz (UCSC) under a letter of authorization from the National Oceanographic and Atmospheric Administration (NOAA). Samples were collected from freshly dead California sea lions including males and females and from a range of life history stages (yearling through adult) who stranded in Monterey Bay between July 2017 and April 2019. Collectively, these specimens and those previously described are 'key taxa' that represent a subset of the Monterey Bay ecosystem, susceptible to DA exposure.

DA Measurements and Isotope Analysis

DA was measured primarily from viscera to obtain information from recently ingested prey (Lefebvre et al., 1999; Gulland, 2000). Liver tissues from stranded sea lions were measured for DA, as they were the only available tissues that offer relatively recent dietary information (days to a couple of weeks) (Vander Zanden et al., 2015). DA was measured from whole body samples of krill and soft tissue in mussels. Approximately 1 gram of unrinsed tissue (to prevent loss of DA because this phycotoxin is water soluble) was combined with 10 mL of 50% methanol. For small individual specimens, including krill and juvenile fish that had minimal soft tissue, viscera from three to eight individuals of the same species collected at a single location were mixed for a combined DA

measurement, as toxin measurements between individuals collected simultaneously are typically similar (Raphael Kudela, pers. comm.). The supernatant from chemical extractions was separated through a 0.2 μm filter and stored at -20°C. To quantify trace levels of DA, the supernatant was processed in a high performance liquid chromatography mass spectrometer (Agilent Technologies 1290 Infinity II 6150 Quadrupole LC/MS) at UCSC, following standard protocols (Mekebri et al., 2009; Peacock et al., 2018).

Muscle tissue and/or whole samples were used for stable isotope analysis. Specifically for krill, muscle and whole body were analyzed from five stations (Stations 110/212; 113; 114; 116; 117; Fig. 1). A linear regression was used to evaluate the relationship between $\delta^{13}C$ and $\delta^{15}N$ from muscle and whole body from stations where both tissues were collected (to determine which krill tissues best represent coastal-pelagic baseline values). Since only whole body was measured from a few stations, these values were converted into that equivalent to muscle using the least-squares regression and are the values used in the subsequent analyses.

Tissues were lyophilized and homogenized into fine powder. To preserve the natural abundances of C and N, and avoid biased trophic links, lipids were not extracted (Murry et al., 2006). C:N ratios were obtained in case the effect of lipid content on C fractionation needed to be corrected (McConnaughey and McRoy, 1979). A total of 1.1 – 1.5 mg of homogenized tissue were weighed into tin capsules. Sample materials were analyzed for bulk analysis at the UC-Davis Stable Isotope Facility using an ANCA-GSL elemental analyzer and PDZ Europe 20-20 isotope ratio mass spectrometer. Isotope compositions are expressed with a δ-notation:

$$\delta\,{}^{H}X = [(({}^{H}X/\,{}^{L}X)_{sample} - ({}^{H}X/\,{}^{L}X)_{standard} / ({}^{H}X/\,{}^{L}X)_{standard})] * 1000,$$

where X is C or N, H is the heavy isotope (^{13}C or ^{15}N), and L is the lighter isotope (^{12}C or ^{13}N). International standards (Pee Dee Belemnite for C and atmospheric N_2 for nitrogen) are applied. Results are expressed as per mil (‰).

Statistical Analyses

Community Structure

To provide insight into food web structure, the average δ^{13}C and δ^{15}N per species and standard error was calculated for all species collected in 2018, and Dungeness crab collected in 2019. Isotope values from sardine and anchovy collected from 2018 and 2019 were included, after interannual differences in isotope values between years were tested using one-way analysis of variance (ANOVA). A convex hull was drawn around the average values of species from each habitat (coastal-pelagic, coastal-benthic, and deep-benthic), which reflects their corresponding isotopic space (Layman et al., 2007). An ANOVA and Tukey Post Hoc Test were used to determine differences in δ^{13}C and δ^{15}N among these three habitats. The habitat characterizations were organized according the cluster analyses on community-habitat relations from the Santora et al. (2012). Coastal-pelagic species feed on the inner continental shelf within the euphotic zone, coastal-benthic species feed in the bottom sediment on the inner continental shelf, and deep-benthic species reside in benthic regions, over the submarine canyon.

DA Concentrations and Isotope Values in Key Taxa Across Habitats

To assess differences in DA accumulation among potential vectors, an ANOVA and a Tukey Post Hoc Test were used with prey species as the factor and DA

concentration as the response variable. Since DA sample distributions were highly skewed, values were $\log_{10}$-transformed. Linear regression analyses evaluated spatial variation in DA, $\delta^{13}C$ and $\delta^{15}N$ as a function of longitude (i.e., to evaluate cross-shore variation). Anchovies were chosen for this DA regression because they are key vectors, can be primary or secondary consumers, and were available at a sufficiently large sample size to evaluate spatial gradients. The average DA value per composite sample at a given station was used. The spatial variability in baseline isotope values was assessed using $\delta^{13}C$ and $\delta^{15}N$ values from krill muscle tissue since they are generally primary consumers and represent basal nutrient sources. These spatial variability regressions incorporated $\delta^{13}C$ and $\delta^{15}N$ from whole body of krill, which were converted into muscle values using the equation $\delta^{13}C_{muscle} = [(\delta^{13}C_{whole} - 6.64) / 1.3069]$. As $\delta^{13}C$ from the whole body in krill increased, muscle $\delta^{13}C$ values increased (Linear Regression, $F_{1,4} = 27.19$, $P = 0.006$, $r^2 = 0.87$). There was no difference between $\delta^{15}N$ from whole body and muscle of krill (Linear Regression, $F_{1,4} = 0.06$, $P = 0.82$, $r^2 = 0.15$).

Trophic Position Estimates and the Isotopic Niche of Key Taxa

Trophic position (TP) estimates were obtained using the equation in Post (2002) for secondary consumers:

$$\text{Trophic Position} = \frac{[(\lambda) + (\delta^{15}N_C - \delta^{15}N_B)]}{\Delta^{15}N_C},$$

where $\delta^{15}N_C$ represents the N value of the secondary consumer identified from isotope analysis. The baseline N value (i.e. mussel for coastal-benthic and krill for coastal-pelagic) and the trophic discrimination factor between a consumer and its prey (3.4‰,

following Post 2002) is represented by $\delta^{15}N_B$ and $\Delta^{15}N$, respectively. The TP of the baseline species is represented with λ. A TP of 2.2 was chosen for krill because it is the average trophic level of *E. pacifica* and *T. spinifera* from the CCS (Miller et al. 2010).

To determine the foraging strategy for each species, the isotope data were analyzed using the isotopic niche framework from Jackson et al., (2011) and Stable Isotope Bayesian Ellipses in R (SIBER) (Jackson and Parnell, 2020). The isotopic niche is represented using Bayesian multivariate standard ellipses, the bivariate equivalent to standard deviation determined through Bayesian probabilities. The ellipses were constructed around each of the eight key taxa and capture 95% of the data points for each species. A total of 100 points from the posterior values returned after 10,000 iterations were used for each ellipse. Anchovy and sardine isotope values from 2018 and 2019 were used together to increase the power of predictive models, as there was minimal interannual variation, and because the ellipse shapes and ranges from 2018 were not altered significantly by adding the 2019 data. Four species of juvenile rockfish were collected and combined for analysis because they occupied similar niche spaces and have overlapping diets (Reilly et al., 1992). The two species of krill were also combined.

To statistically compare the size of each isotopic niche, Bayesian standardized ellipse areas (SEA_b) were calculated and compared using the 95% credible intervals (CI). To evaluate differences in diet and habitat, niche overlap among species was calculated by quantifying the maximum likelihood overlap between the 95% prediction ellipses. The overlap is expressed as a proportion of the non-overlapping area of two species, which provides output values ranging from 0 (distinct ellipses) to 1 (complete overlap) (Jackson and Parnell, 2020). The output values representing the proportion of non-overlapping

area was multiplied by 100 and expressed as a percent. Each of the percent proportions of overlap reflect distinct feeding strategies, diet, and habitat use.

To reduce the effect of spatial variability on baseline isotope values and better evaluate foraging strategies, specifically regarding habitat use, a 'site-control analysis' was completed. This analysis consisted of the same SIBER quantifications described above; however, it was limited to a subset of individuals collected from three adjacent stations just south of the Monterey Canyon (Fig. 1). A decline in SEA_b size and change in ellipse shape between the full and site-control analysis for animals with minimal mobility may indicate that the original ellipse area was influenced by heterogeneity in baseline isotope values and individual variability in diet. In contrast, no change in SEA_b size and ellipse shape would indicate that specimens were comprised of individual specialist feeders belonging to a subpopulation of generalists. Sea lions were not used in the site-control analysis because each individual was collected from a different stranding location in Monterey Bay, and whether they were residents to the region remains unknown. Mussels were excluded because of their low sample size.

Finally, the isotopic space that potential and active vectors occupy within the broader community was calculated using the SIBER framework. Bayesian standard ellipses were calculated for (i) all potential vectors (using each isotope value regardless of taxa; SEA_{DA}), (ii) active vectors (SEA_A), and (iii) all individual specimens collected, which represents the subsampled community in Monterey Bay (SEA_{MB}). To compare the isotopic spaces of the potential and active DA vectors with the larger community, the

proportion of the SEA_{MB} represented by SEA_{DA} (and SEA_A) was calculated using the percentage overlap statistics described previously.

RESULTS

Sample Collection

A total of 22 fish and invertebrate species covering a range of trophic levels were collected from 13 sites (Fig. 1; Table 1; Appendix T1). The analysis consisted of 183 specimens representing 21 species collected in 2018, and 21 sardines, 21 anchovies, and 29 Dungeness crabs collected in 2019. There were no differences in $\delta^{15}N$ values between the 2018 and 2019 collections for sardines (ANOVA $F_{1,27} = 0.65$, $P = 0.8$) or anchovies ($F_{1,67} = 0.6$, $P = 0.4$ for anchovies) and the shape and size of their ellipses did not change across years, thus specimens were pooled for isotope analyses.

Community Structure and Potential DA Vectors

Figure 2a illustrates the mean $\delta^{13}C$ and $\delta^{15}N$ values for each species. Each convex hull encompasses discrete isotope values comprised by species in each habitat. A total of four species were classified as deep-benthic, six as coastal-benthic, and ten as coastal-pelagic. The coastal-pelagic convex hull area was smaller than coastal-benthic and had a relatively narrow range in $\delta^{13}C$ (2.12‰) (Fig. 2a). All potential DA vectors, except mussels, occupied the relatively narrow range of $\delta^{13}C$ values for species feeding in coastal-pelagic habitats (difference in $\delta^{13}C$ between krill and sardines, the two extremes). The mean isotope values of potential vectors were depleted in $\delta^{13}C$ and $\delta^{15}N$ by ~2‰ and ~4‰ compared to the average sea lion (Fig. 2a). There was

overlap between coastal-benthic and coastal-pelagic convex hulls, but the isotope values of each species within each habitat were significantly different among them (Fig. 2a; ANOVA, $F_{3,242} = 79.01$, $P < 0.001$ for $\delta^{13}C$; ANOVA $F_{3,242} = 22.35$, $P < 0.001$ for $\delta^{15}N$). The average deep-benthic species, including octopus, spotted ratfish, CA grenadier, and combfish, were depleted by 1.88‰ in $\delta^{13}C$ and enriched in $\delta^{15}N$ by 2.87‰ compared to coastal-benthic species (Tukey HSD < 0.001 for $\delta^{13}C$ and $\delta^{15}N$; Fig. 2a). The average coastal-pelagic species were depleted by 0.74‰ for $\delta^{13}C$ and 3.14‰ for $\delta^{15}N$ relative to the deep-benthic (Tukey HSD < 0.001 for $\delta^{15}N$ and Tukey HSD > 0.05 for $\delta^{13}C$) and depleted by 2.62‰ and 0.27‰ for $\delta^{13}C$ and $\delta^{15}N$ relative to coastal-benthic convex hulls (Tukey HSD < 0.001 for $\delta^{13}C$ and $\delta^{15}N$).

The Bayesian metrics revealed that the six potential DA vectors occupied ~40% of the community represented in this study (Fig. 2b). These DA vectors have lower trophic positions and occupy the lower half of the $\delta^{15}N$ values from the ellipse (Fig 2b; Table 1). Anchovies collected in the 2018 sampling period comprised 7.96% of the community's ellipse area.

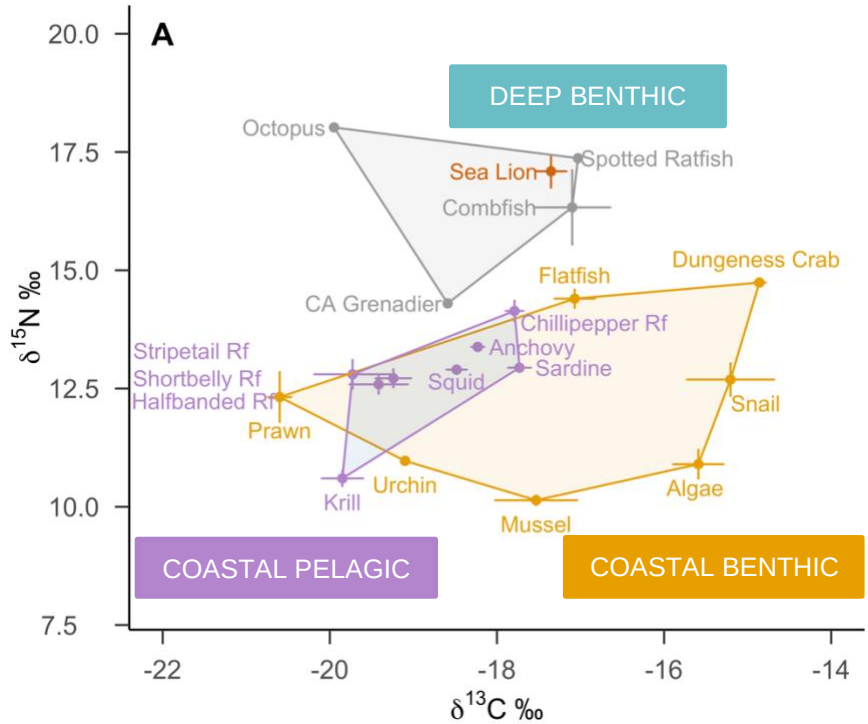

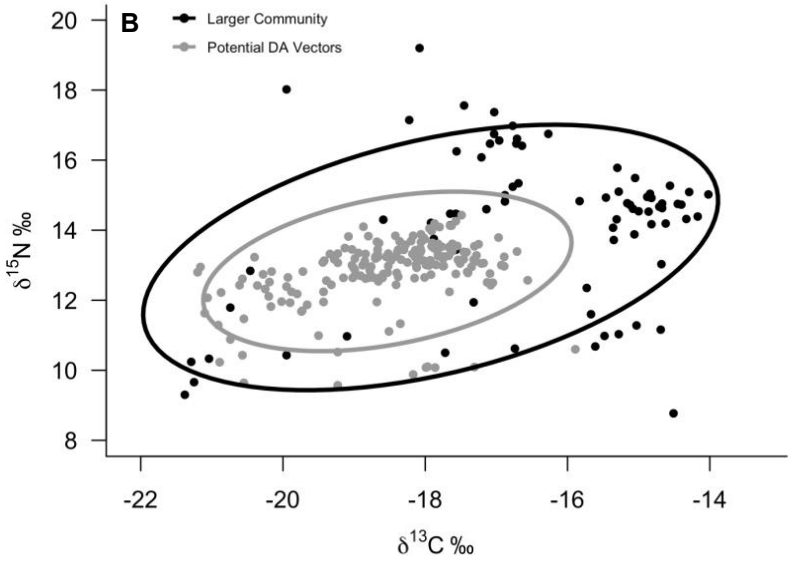

Figure 2. Community structure. (A) The average $\delta^{13}C$ (‰) and $\delta^{15}N$ (‰) values of all species collected in Monterey Bay in 2018 and 2019. Each point represents the mean value for each species (± 1 standard error). Convex hulls surround the mean values of species in their corresponding habitat: coastal-benthic in orange, coastal-pelagic in purple, deep-benthic in grey. Stranded sea lions were excluded from convex hulls because they can feed on prey from any of these habitats. Rf refers to rockfish. (B) Comparison of Bayesian standard ellipses between the whole community (all specimens analyzed in this study; black) and the six potential DA vectors (grey). Each point represents the isotope value per individual.

DA Concentrations and Isotope Values From Key Taxa Across Habitats

DA concentrations ([DA]; ppm) were limited to samples collected in 2018. No Dungeness crabs were analyzed. Potential DA vectors exhibited differences in [DA] in their viscera (ANOVA, $F_{5,50} = 19.8$, $P < 0.001$). Anchovies accumulated the highest [DA] (and had the greatest variance) compared to other species (Fig. 3) and were the only species exceeding the active vector threshold for protecting human health (Tukey HSD, $P < 0.001$). Anchovies from a single collection site had an average [DA] of 15.03 ppm, which is 10x greater than that accumulated in any other potential vector species (Fig. 3;

Appendix T1). Sardines recorded the second highest average [DA], and krill accumulated the least DA among potential vector species (Fig. 3). Juvenile rockfish, market squid, and mussels recorded similarly low levels of DA, ranging from 0.21 to 0.29 ppm (Fig. 3). Sea lion livers contained the least [DA] of all taxa and tissue types in the years that I sampled (Fig. 3).

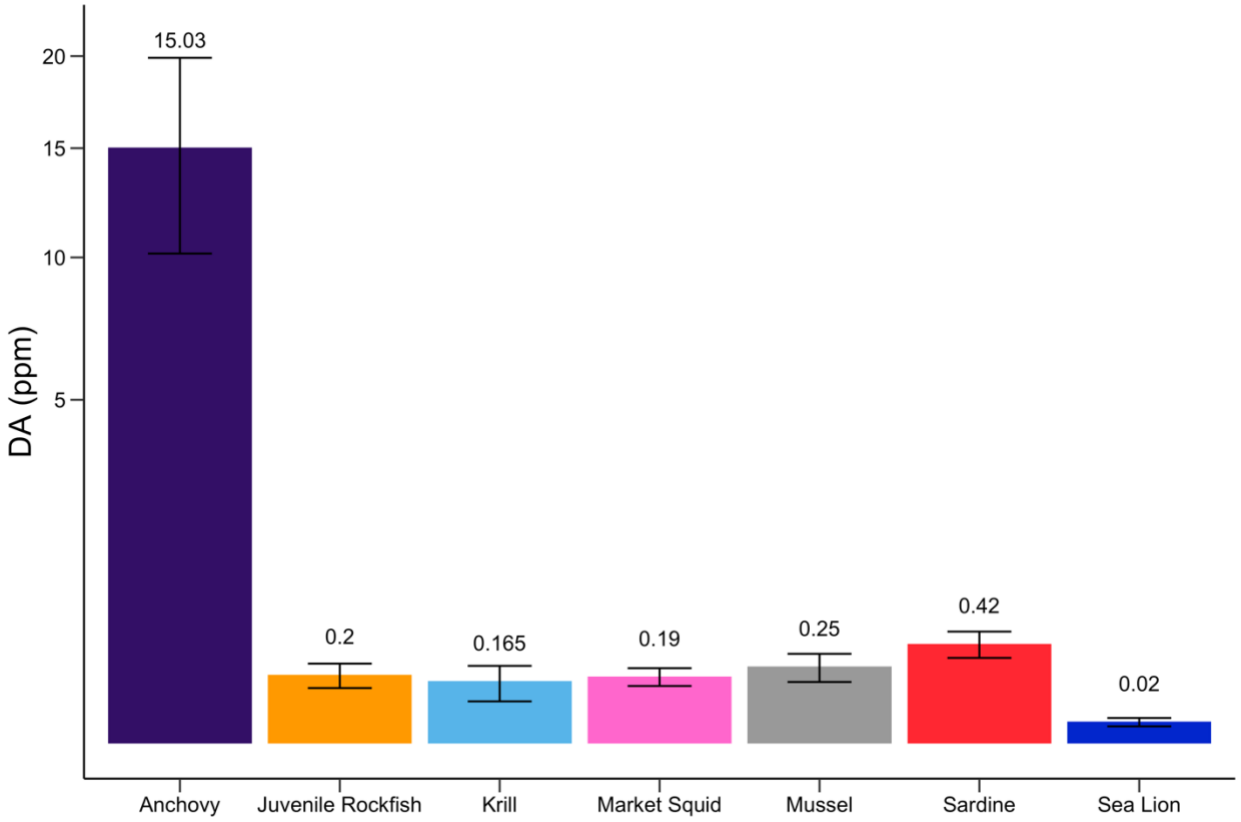

Figure 3. DA Measurements Among Key Taxa. The average DA concentrations (ppm) of potential DA vectors and predators known to be susceptible to DA toxicosis. Error bars represent ± 1 standard error.

A negative relationship between DA accumulation in anchovies and longitude (representing a coastal to offshore gradient) was documented: anchovies collected at central and southern sampling sites inside Monterey Bay had higher [DA] than those further offshore (Linear Regression, $F_{1,6} = 5.75$, $P = 0.05$, $r^2 = 0.48$; Fig. 4a). There was

also a negative linear relationship between $\delta^{13}C$ in krill and longitude (Linear Regression, $F_{1,5} = 12.8$, $P = 0.03$, $r^2 = 0.63$; Fig. 4b), such that krill collected from inshore stations had higher $\delta^{13}C$ values. The $\delta^{15}N$ in krill did not vary with longitude (Linear Regression, $F_{1,5} = 0.015$, $P = 0.9$, $r^2 = 0.01$).

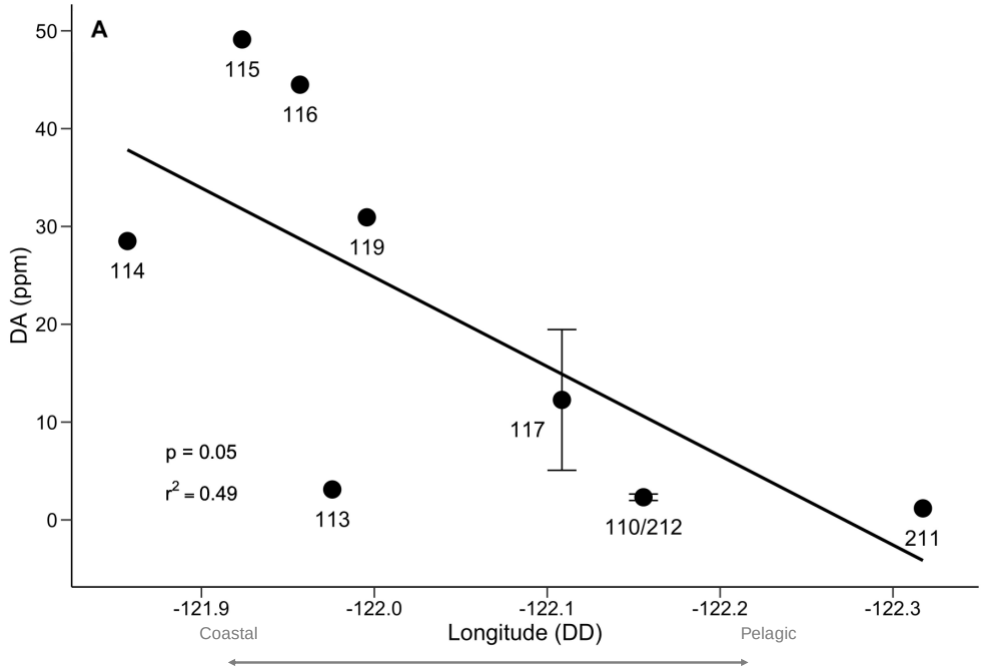

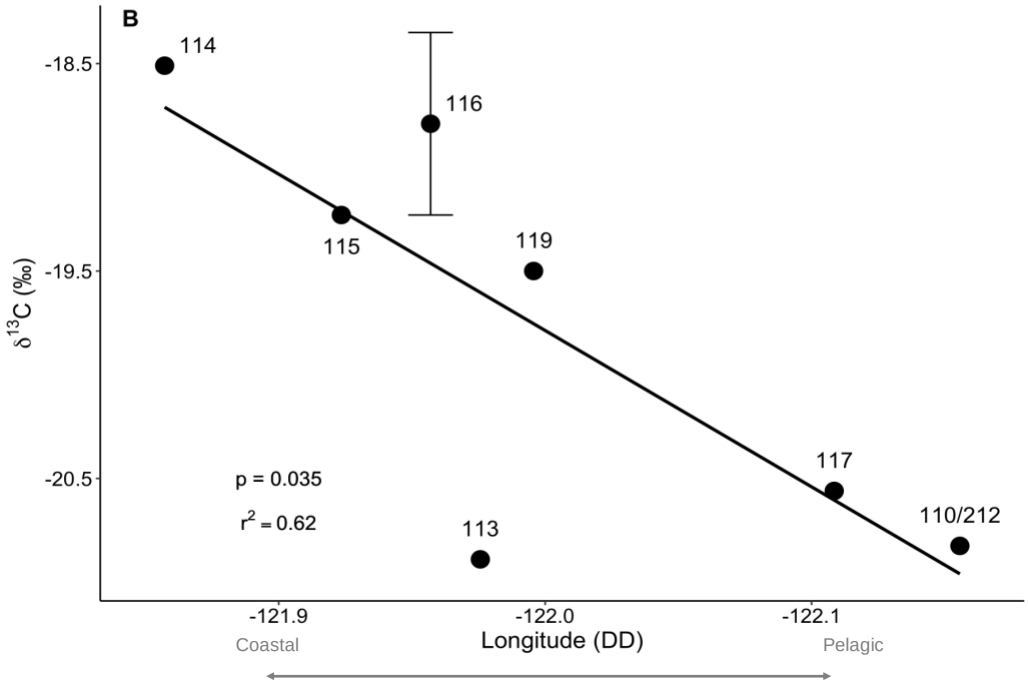

Figure 4. Spatial Variation in DA and Baseline Isotope Values. Regression analyses showing the association between (A) the average DA concentrations (ppm) of anchovies and longitude of collection site and (B) the average $\delta^{13}C$ (‰) from muscle tissue in krill and longitude. Station numbers correspond to those depicted in Fig. 1. Error bars represent standard error at stations with multiple samples.

Isotopic Niche, Trophic Position, and DA Accumulation of Key Taxa

Among DA vectors, anchovies and market squid had the highest degree of ellipse overlap (50%), followed by market squid and sardines (46.23%), anchovies and sardines (40%), and market squid and juvenile rockfish (38.5%) (Fig. 5a, Appendix T5). These four species occupied similar isotopic niches and had similar average $\delta^{15}N$ values and trophic positions (Fig 5a,c; Table 1). The smallest degree of overlap was between juvenile rockfish and market squid, and market squid and krill (13.8% and 4.19%; Appendix T5). Krill did not overlap with sardines nor anchovies (Fig. 5a). Even though anchovies and market squid overlapped by 50% (Fig. 5a), market squid accumulated the

least DA (0.19 ppm) of all coastal-pelagic foragers, while anchovies accumulated the most (Fig 3; Fig. 5a; Appendix T1).

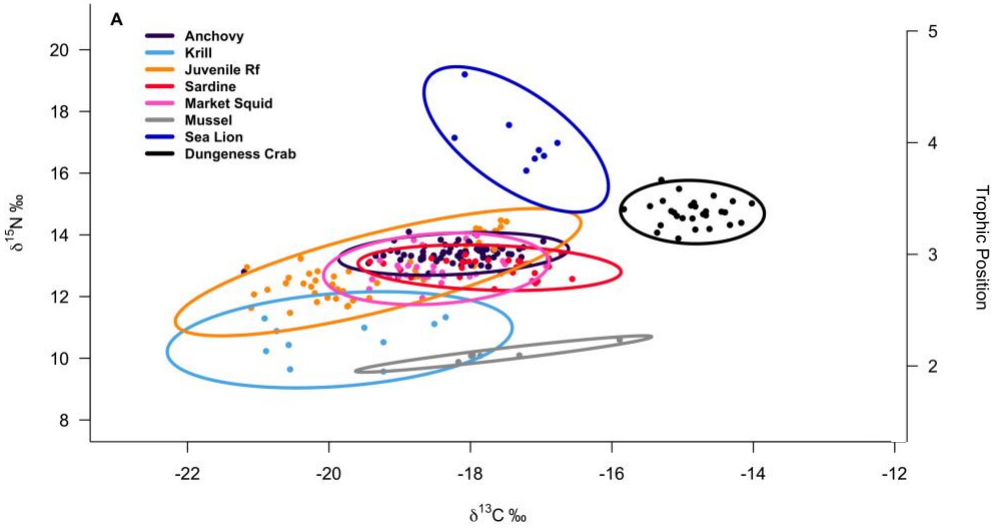

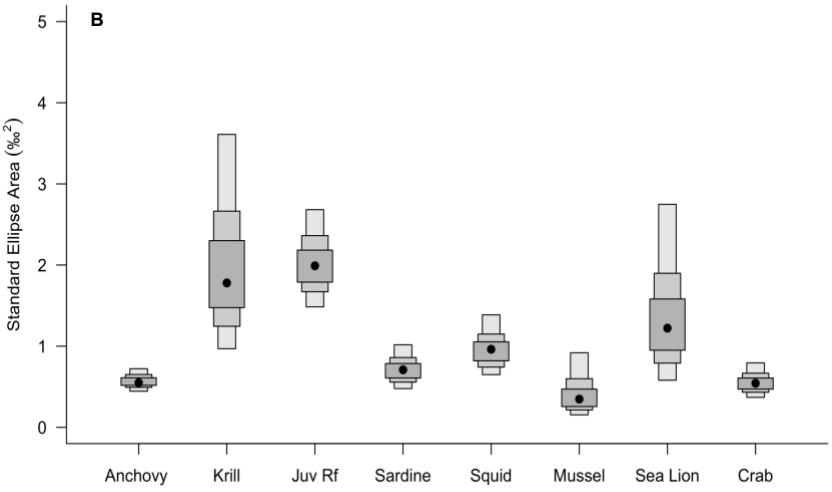

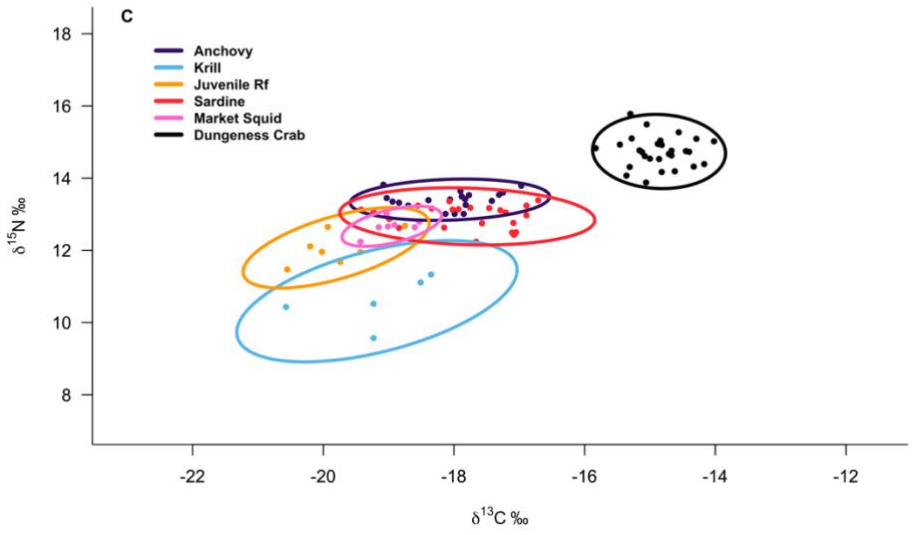

Figure 5. Isotopic Niches of Key Taxa. (A) Bayesian standard ellipses and trophic level estimates of key taxa. Each point represents an individual. (B) The Bayesian ellipse area (SEA_b) per species and 95% confidence interval. Black dots represent the mean SEA_b after 10,000 iterations. The surrounding shaded density plots represent the 50%, 75%, and 95% credible intervals. (C) Site-control analysis presenting the Bayesian ellipses of five potential DA vectors collected at stations 114, 115, and 116, and Dungeness crabs at C1 and C2 (see Fig. 1).

Sardines and anchovies reflected similar trophic positions and were characterized by ellipses that were moderately wide, with narrow ranges of $\delta^{15}N$ that resulted in a compressed isotopic niche (Fig. 5a,c; Table 1). The shape of their ellipse remained similar when datapoints were reduced in the site-control analysis (Fig. 5a,c). Anchovies had a slightly higher raw mean and smaller variance in SEA_b than sardines and accumulated significantly more DA (Fig. 5b; Fig. 3; Appendix T1,2,4). Results from the raw mean SEA_b (without considering the 95% CI) showed that anchovies and sardines have smaller SEA_b than market squid or moderately mobile species like krill and juvenile rockfish (Fig. 5b; Appendix T1,2,4).

As baselines indicators, mussel and krill ellipses exhibit the widest range of $\delta^{13}C$ values (~6‰ and >5‰) (Fig. 5a). Mussels contained the third highest DA concentration (Fig. 3), the lowest $\delta^{15}N$ values and trophic position among potential vectors, and the narrowest range in $\delta^{15}N$ (< 1‰), leading to the most compressed ellipse among taxa (Fig. 5a). Based on the 95% credible intervals, average SEA_b values of mussels are similar to that of krill, but smaller than sardines and anchovies (Fig. 5b; Appendix T4). The wide range in $\delta^{13}C$ and $\delta^{15}N$ values for muscle in krill is consistent with it occupying the second largest SEA_b, although they have the least DA of all potential vectors and the lowest trophic position among the pelagic vectors (Fig. 3; Fig. 5a). While the range in $\delta^{13}C$ appears to be reduced between the full and site-control analysis, the mean SEA_b, and shape and orientation of the krill ellipse did not change (Fig. 5a,c; Appendix T4,6).

The trophic position estimate for juvenile rockfish was comparable to market squid, but market squid had a narrower $\delta^{15}N$ range (Table 1; Fig. 5a). The juvenile rockfish ellipse exhibited the largest range in $\delta^{15}N$ (~4.5‰) of the potential DA vectors and a wide range in $\delta^{13}C$ values (~6‰), resulting in the highest mean SEA_b (Table 1; Fig. 5a). Their mean SEA_b declined from 2.18 with the full dataset to 0.81 in the site-control analysis (Fig. Fig. 5; Appendix T4,6). Market squid had a relatively small mean SEA_b that also declined from 0.7 in the full analysis to 0.13 in the site-control analysis (Appendix T4,6).

Dungeness crabs had a round ellipse with similar $\delta^{13}C$ and $\delta^{15}N$ ranges (Fig. 5a,c). The SEA_b for crabs is comparable to that for sardines and anchovies despite their higher trophic position (Table 1; Fig. 5b; Appendix T4). Stranded sea lions contained the least DA and occupied the highest trophic level (Fig. 3; Table 1; Appendix T1). They are enriched by ~3-4‰ in $\delta^{15}N$ compared to the mid-trophic foragers and possess an ellipse with the greatest range in $\delta^{15}N$ (~6‰) (Fig 5a). Unlike the potential DA vectors and Dungeness crabs, sea lions have a wider range in $\delta^{15}N$ than $\delta^{13}C$, resulting in a more vertically shaped ellipse (Fig. 5a).

DISCUSSION

This is the first study to present a combined approach using isotope analysis and DA measurements to evaluate variability in DA accumulation across habitats, species, and trophic levels. Below, I discuss isotope results from all specimens collected in 2018 and 2019, the variation in DA accumulation, and then interpret the feeding strategies of key taxa. My study provides insight into the community structure and different baseline isotope values among habitats, highlights inshore-offshore gradients in isotope values and DA accumulation in Monterey Bay, and reveals differences in toxin accumulation and foraging strategy across taxa. These results have implications for reconstructing the food web and for identifying routes of DA trophic transfer.

Variation in Baseline Isotope Values Reveals Differences in Community Structure and Biochemical Processes Among Habitats

The isotopic differences among the three convex hulls suggests that distinct elemental cycling processes dominate in each habitat, driving unique baseline C and N isotope values. The wide range in $\delta^{13}C$ for the coastal-benthic convex hull (5.7‰) could be driven by a mix of carbon sources and primary productivity derived from terrestrial, estuarine, and marine systems (Peterson and Fry, 1987). The coastal-pelagic zone had the narrowest convex hull (2.12‰); however, krill from these habitats reflect a significant onshore-offshore gradient in $\delta^{13}C$, with longitude explaining 63% of this spatial variation (Fig. 2a, 4b). Krill collected from lower longitudes, at central and southern stations inside Monterey Bay had higher $\delta^{13}C$ values than those in pelagic zones. Since krill are primary consumers and are not thought to actively move horizontally, and because there is minimal fractionation of $\delta^{13}C$ during respiration and dietary consumption (DeNiro and Epstein, 1978), krill likely reflect source information integrated from the water mass in which they reside. Thus, suggesting differences in C cycling from the coastline and throughout coastal-pelagic regions within Monterey Bay. The observed negative gradient in $\delta^{13}C$ is not necessarily influenced by C input from terrestrial systems. Secondary isotopic fractionation from terrestrial input is not likely a dominating factor, as previous studies on $\delta^{13}C$ from plankton in Monterey Bay document no correlation between salinity (which should decrease from river runoff and terrestrial C inputs) and $\delta^{13}C$ of particulate organic carbon in surface waters (Rau et al., 2001).

Rather, the higher $\delta^{13}C$ values observed in krill from inside Monterey Bay may result from variation in species composition of primary producers. Primary producers and autotrophs, including phytoplankton, fix carbon. Depending on the species of phytoplankton, and its size, growth rate, and preferred photosynthetic pathway, there is a varying degree of isotopic fractionation (Smith and Epstein, 1971; Peterson and Fry, 1987). Larger cell phytoplankton, such as *Pseudo-nitzschia* diatoms, have faster growth rates and are enriched in ^{13}C, and thus have higher $\delta^{13}C$ compared to slower growing, smaller phytoplankton (Goericke and Fry, 1994). The water inside Monterey Bay provides the necessary nutrients to support larger biomass phytoplankton (Wilkerson et al., 2001). This results from local circulation patterns. More specifically, during seasonal upwelling, bands of newly outcropped, nutrient rich water move from Año Nuevo towards Point Lobos and Carmel and bifurcates (Rosenfeld et al., 1994). Some of this water remains trapped inside Monterey Bay because of the cyclonic gyres (Paduan and Rosenfeld, 1996), allowing larger celled phytoplankton to thrive, thus yielding higher $\delta^{13}C$ values. In contrast, water masses outside the mouth of Monterey Bay on the other side of the bifurcated flow are less productive and favor lower biomass primary producers with lower $\delta^{13}C$ values (Rosenfeld et al., 1994; Paduan and Rosenfeld 2001; Wilkerson et al., 2001). The differences in productivity that contribute to inshore versus offshore gradients and spatial heterogeneity in $\delta^{13}C$ have similarly been documented in other marine environments (Burton and Koch, 1999; Schell et al., 1998).

The oceanographic forces and productivity gradients that influence spatial variability in $\delta^{13}C$ may also contribute to the decoupling of inshore and offshore blooms. In fact, the four groups of anchovies that accumulated >20 ppm were collected inside

Monterey Bay, at sites where krill were enriched in ^{13}C (albeit $\delta^{13}C$ from krill may capture a different integration time than accumulation of DA in viscera) (Fig. 1,4; Appendix T2). The nutrient rich water from seasonal upwelling that remains trapped inside Monterey Bay continually recirculates (Paduan and Rosenfeld, 1996), and with high nitrate concentrations, fuels toxic producing blooms. On the other hand, water masses outside the mouth of Monterey Bay receive greater influence from the larger moving CCS, move faster, and circulate in a less cyclical manner, creating conditions less favorable for *Pseudo-nitzschia* blooms (Rosenfeld et al., 1994; Paduan and Rosenfeld 2001). Since DA-producing *Pseudo-nitzschia* blooms are sensitive to small-scale oceanographic features (Ryan et al., 2005, 2014; Trainer et al., 2012; Lewitus et al., 2012), it may be possible for enriched ^{13}C values in regions inside of Monterey Bay (or the oceanographic forces that lead to such differences*)* to be characteristic of toxic *Pseudo-nitzschia* blooms.

The bifurcated flow of water separating Monterey Bay from the larger CCS that contributes to spatial heterogeneity in $\delta^{13}C$ and toxic forming HABs may explain why station 113 is a consistent outlier in the spatial analyses (Fig. 4). Station 113 has krill with lower $\delta^{13}C$ values and DA accumulation in anchovies, and is geographically situated at a boundary between the inner shelf inside Monterey Bay and the dynamic upwelling zone (Santora et al., 2012). It may experience different enviornmental conditions than other stations because it is highly influenced by upwelled water that is transported across the mouth of Monterey Bay and newly outcropped at Point Lobos. This upwelled water is depleted in ^{13}C and has lower $\delta^{13}C$ signatures because of photosynthetic processes occuring in surface waters: as phytoplankton with low $\delta^{13}C$ sink and accumulate at depth,

it remineralizes and the water outcropping reflects the lower $\delta^{13}C$ values. The upwelled water may also create more turbulent conditions than sites on either side of the bifurcated tongue, creating unfavorable conditions for HAB events and DA production.

Different $\delta^{15}N$ values among species and convex hulls implies that these habitats are dominated by distinct N sources and cycling processes, because $\delta^{15}N$ of marine species reflect information on their diet and foraging habitats (Ruiz-Cooley et al., 2012). Octopus and ratfish had higher $\delta^{15}N$ values than their potential predator, the sea lion (Fig. 2a). Rather than octopus feeding at higher trophic levels than sea lions, which is consistent with the assumption that $\delta^{15}N$ increases with trophic level (Minagawa and Wada, 1984), these findings suggest variation in baseline $\delta^{15}N$ values between deep-benthic and the coastal habitats. Deeper waters are usually enriched in N by up to 5-10‰ because ^{14}N is lost faster than ^{15}N during particulate N decomposition at depth, as identified in the northeast Indian Ocean (Saino and Hattori, 1980; Peterson and Fry, 1987). Such ^{15}N enrichment in deeper habitats may be associated with remote upwelling sources from the northward moving California undercurrent that influences depths >30 m in Monterey Bay (Liu and Kaplan, 1989; Altabet et al., 1999). Since deep-benthic regions are enriched in ^{15}N, so will the consumers foraging in such habitats. Therefore, $\delta^{15}N$ values from consumers feeding in coastal-pelagic, deep-benthic, or coastal-benthic regions (from tissues with fast turnover rates such as blood or liver, reflecting information from the most recently ingested meal) could help identify the foraging grounds of mobile animals containing DA, including stranded marine mammals with DA toxicosis.

Variation in DA Accumulation Across Habitats and Taxa

Small pelagic fish accumulated higher concentrations of DA than taxa from other habitats (Fig. 3). Benthic invertebrates and flatfish species had minimal DA in their viscera (Appendix T1), which may have been acquired from toxic sinking particulate matter, including *Pseudo-nitzschia* spp. cells or fecal pellets from planktivorous feeders, or through resuspending and ingesting toxins that accumulated in the sediment from previous DA events (Lefebvre et al., 2002a; Vigilant and Silver, 2007). It is also known that toxic cells rapidly flocculate to the seafloor (Sekula-Wood et al., 2009; Umhau et al., 2018). Yet, anchovies contained high DA concentrations in their viscera, suggesting that newly produced toxic blooms were likely present in the water column where they fed, despite the lack of DA detected by routine CDPH shore monitoring and no documented region-wide blooms within the region of study and time frame (Thompson et al., 2018; Harvey et al., 2019; R. Kudela, pers. comm). Anchovies potentially accumulated toxins from directly ingesting toxic cells in cryptic subsurface layers (McManus et al., 2008), given that DA was not present in krill, considered an intermediary source of DA. Anchovies were also the only species with DA concentrations exceeding the federal regulatory limits (20 ppm), indicating that, at times, they may be the most powerful DA vector in coastal-pelagic, upwelling regions such as Monterey Bay. Their role as a DA vector could result from their foraging strategies described below.

The differences in DA accumulation between anchovies and mussels are consistent with previously observed decoupling between offshore and nearshore coastal environments in the southern CCS (Kudela et al., 2012; Frolov et al., 2013, Umhau et al. 2018). The spatial mismatches and patchy distribution of HAB species and DA

production renders ‘fixed point’ nearshore monitoring, like that used for mussels, insufficient for identifying presence or absence of DA in the CCS given the incredibly dynamic coastal processes that characterize hotspots, including the Monterey Bay (Ryan et al., 2011). My findings confirm these claims: anchovies collected on May 15 and 16, 2018 contained 28 to 49 ppm DA, while mussels from the SCW on the same date only contained 0.42 ppm (R. Kudela, unpublished data). Anchovies, like mussels, capture instantaneous shifts in the environment because DA in their viscera represents recently ingested toxins (Lefebvre et al., 2002b). Collectively, my results indicate that anchovies are good indicators of DA in non-coastal waters where routine shoreline monitoring initiatives would fail to detect these events, highlighting the limitations of relying on mussels as the only or primary indicator species for DA presence in a given ecosystem.

The longitudinal gradient observed in DA accumulation in anchovies reflects similar patterns in phytoplankton composition data and DA levels identified from prior studies. In 1998, 2013, and 2015, years characterized by El Niño conditions and extremely toxic DA outbreaks, adaptive sampling techniques recording phytoplankton community composition and quantifying toxin levels documented the highest pDA concentrations in the central and southern regions of Monterey Bay (Trainer et al., 2000; Bowers et al., 2018), near stations 114-116 and 119, the sites where anchovies accumulated the highest DA levels in the current study. Reports from non-El Niño years found similar spatial variability and heterogeneity in phytoplankton composition and DA levels, and point to small-scale variability in wind-driven upwelling as the primary driving force in toxic HAB outbreaks (Ryan et al., 2011). It is possible that central and southern stations inside Monterey Bay, where anchovies with high amounts of DA were

collected, were exposed to toxic blooms from nutrient intrusions that did not otherwise impact sites in the upwelling shadow (Graham and Largier, 1997) or along the coastline.

Minimal DA was detected in liver samples from sea lions (Fig 3). Liver is not the optimal tissue to detect DA (Gulland, 2000), but was selected for this analysis because it reflects recent dietary sources (over a scale of days) and was readily available. The trace levels of DA in sea lion livers are consistent with their necropsy reports indicating no signs of DA toxicosis (R. Dunkin, pers. comm.). It also aligns with findings from sea lions over a geographic range extending beyond Monterey Bay (Greig et al., 2005; Goldstein et al., 2008). The number of admitted sea lions in central California with confirmed or suspected DA toxicosis symptoms in 2018 was close to the median number of animals, relative to a 1998-2019 baseline (C. Field, TMMC, pers. comm.), suggesting that the populations of sea lions in these regions were not exposed to particularly high DA levels during the study period.

Isotopic Niche and DA Concentrations Reveal the Foraging Strategies of Key Vector Species

The foraging strategy (i.e. dietary and habitat generalist or specialist) of key taxa was determined using the size (SEA_b), shape, and orientation of each species' isotopic niche and ellipse. A relatively small SEA_b with a narrow range in $\delta^{15}N$ and wide range in $\delta^{13}C$ values, resulting in a flat, compressed ellipse indicates a dietary specialist feeding at sites with different C sources (Layman et al., 2007). Controlled laboratory experiments suggest that diet generalists may have a small SEA_b and a round ellipse with narrow ranges in $\delta^{13}C$ and $\delta^{15}N$ from integrating prey of different trophic levels (Flaherty and

Ben-David, 2010). In the wild, a small SEA_b may indicate a group of specialist feeders that integrates source information from similar prey and habitat types. A broad isotopic niche in the wild, with a relatively large SEA_b and greater range in $\delta^{15}N$ values than $\delta^{13}C$ may reflect highly mobile individuals who have distinct diets and forage in regions with variable baseline isotope values, thus supporting a population of generalists (Layman et al., 2007; Newsome et al., 2009). Habitat generalists that are diet specialists may display a narrower niche width and smaller SEA_b than habitat specialists because generalists integrate prey and nutrients from a variety of baseline source values (Flaherty and Ben-David, 2010). These classifications were used in conjunction with known information on the diet and feeding capacity to interpret the foraging strategy for key taxa.

Mussels had the most compressed ellipse of all potential vectors, indicating diet specialization, a strategy for sessile mollusks whereby they only consume microorganisms of a particular size class and detritus suspended in the water column at their site of attachment (Fox and Coe, 1943). The wide range in $\delta^{13}C$ results from mussels being collected at two locations with different primary producers and C inputs. Similar to $\delta^{13}C$ being a site-specific signal, DA concentrations from mussels are also site-specific because mussels are sessile and accumulate and depurate DA faster than other bivalves (Novaczek et al., 1992; Wohlgeschaffen et al., 1992). While they are good sentinels for public health at a local scale, my results indicate that they did not capture toxins during low DA years nor the C or N sources that are further offshore (Fig. 3).

Unlike mussels, Dungeness crabs have a round ellipse that suggests a generalist diet. Their round ellipse may result from their capacity to consume a broad array of

teleost fish and crustaceans from the benthos (Stevens et al., 1982) and move between coastal-benthic and deeper habitats, depending on life stage. Dungeness crabs could be potential predators of mussels (Stevens et al., 1982), indicated by an enrichment in δ^{15}N by ~4‰. The isotopic niche data supports that krill, market squid, and juvenile rockfish, among coastal-pelagic DA vectors, are diet generalists at a population level. The isotopic niche of krill and consistency in niche shape and size between the site-control and full analysis reflects the fact that krill are restricted to feeding within a defined water mass. While krill feed opportunistically, their limited mobility (Brinton, 1962; Gómez-Gutiérrez et al., 2005; Cimino et al., 2020) prevents them from capturing toxins from as broad a region in coastal-pelagic zones as highly mobile foragers, such as anchovies, or from being proxies for a single habitat as seen for mussels.

Market squid and juvenile rockfish ellipses declined between the full and site-control analysis, primarily by a reduced range in δ^{13}C and a small decline in δ^{15}N . This may indicate that their original SEA_b was partially driven by specimens being collected from multiple geographic regions with varying baseline values or from differences in diet among individuals at each site. The reduced ellipse for market squid in the site-control analysis suggests that individuals from the same collection site fed on prey from a single trophic level and region, which is consistent with previous studies: market squid primarily are restricted to feeding in a single water mass and feed on dense patches of krill, copepods, and megalop larvae (Karpov and Cailliet, 1979; Ish et al., 2004). Juvenile rockfish may be less mobile than squid, but are also opportunistic in that they consume pelagic copepods, krill, and krill eggs, depending on what is seasonally abundant (Reilly et al., 1992). The juvenile rockfish may represent a planktivorous foraging guild of

generalist individuals who consume available prey, as they had a wide, ~3‰ range in δ^{15}N. Interestingly, market squid and juvenile rockfish had minimal toxins, even from hauls where anchovies detected high [DA], suggesting that despite their ability to accumulate DA in Monterey Bay (Bargu et al., 2002, 2008), they were not important vectors in the years sampled here.

The isotopic niche data from anchovies and sardines suggest that they are both dietary and habitat specialists, likely feeding across a wide geographic range along the coastline. Anchovies and sardines migrate extensively between spawning locations and pelagic feeding sites, and integrate nutrient sources from diverse regions through their diet (Van Der Lingen et al., 2009). The overlap in isotopic space (40%) between sardines and anchovies and similar ellipse size, shape, and trophic positions support that they have similar foraging strategies; however, the lack of overlap (60%) in their ellipses and their differences in DA levels indicate an important degree of resource partitioning at the baseline level. This resource portioning may result from morphological restrictions: anchovies are size-selective, particulate feeders with coarse gill rakers who preferentially ingest larger prey (compared to sardines), including larger copepods and phytoplankton (Van Der Lingen et al., 2009). They thrive in nutrient rich, highly turbid, upwelled water that supports large-celled diatoms, including toxin-producing *Pseudo-nitzschia* spp. (Rykaczewski and Checkley, 2008). Toxic *Pseudo-nitzschia* spp. may be ingested directly by anchovies (Lefebvre et al. 2002b) or indirectly through copepods containing DA (Bargu et al., 2002). Toxic *Pseudo-nitzschia* cells may be less available to sardines. The primary feeding mode for sardines is non-selective filter-feeding on smaller sized plankton because they have finer gill rakers than anchovies (Van Der Lingen et al.,

2006). Such morphological restrictions in sardines make it more energetically efficient to inhabit regions with warmer environments that support smaller phytoplankton (i.e. dinoflagellates) incapable of producing DA and supporting smaller zooplankton.

The finding that anchovies were more efficient DA vectors than sardines because of resource partitioning during a period without high levels of reported toxins is consistent with Lefebvre et al. (2002b). These authors found that *Pseudo-nitzschia* spp. cell densities and DA levels were twice as high in anchovies compared to sardines collected simultaneously in Monterey Bay between 1999 and 2000 and suggested that anchovies were feeding exclusively on diatoms, while sardines were feeding on zooplankton with lower DA concentrations. More recent research indicates that sardines and anchovies are opportunistic foragers, partition prey based on size class, and occupy different trophic positions (Van Der Lingen et al., 2006; Miller and Brodeur, 2007; Checkley et al. 2009). My results partially disagree with these findings: the selection of prey based on size explains their distinct capacities to accumulate DA, but both species occupy the same trophic level.

The isotopic niche data for sea lions and ability to forage across large spatial scales suggests that they have generalist tendencies, potentially at a subpopulation level. The stranded sea lions could be from a broader population of mobile individuals that integrate source information from a range of habitats and prey throughout the CCS, driving their wide range in $\delta^{13}C$ and $\delta^{15}N$ between individuals. Sea lions may be individual specialists who opportunistically exploit seasonally abundant prey and forage throughout the continental shelf, integrating a variety of baseline N values (Lowry et al., 1991; Weise and Harvey, 2008). This would explain the vertically shaped ellipse, cluster

of individuals with similar isotope values with outliers, and high variance in SEA_b. The variance could also result from a heterogenous sampling scheme that encompassed male and female individuals who forage between 90 and 650 km from shore (Costa et al., 2007) and may not be residents of Monterey Bay. Given the high mobility of sea lions and that an individual may opportunistically feed over broad spatial scales, it may be difficult to use sea lions as a sentinel species for DA warnings at the local scale, but they are extremely useful for capturing broad ecosystem-level variability in phycotoxin production and impact.

SUMMARY & MANAGEMENT IMPLICATIONS

The ability to predict and respond quickly to HAB events and manage human health and wildlife threats requires knowledge of the main DA vectors and their foraging patterns, especially in regional hotspots for DA outbreaks. This study illustrates the efficacy of using DA measurements from tissues with fast turnover rates, and $\delta^{13}C$ and $\delta^{15}N$ from bulk tissue samples of a wide range of taxa, to identify the main vectors of DA transfer during a period without coast-wide toxic blooms nor highly anomalous oceanographic conditions. Ultimately, this approach allowed me to determine the habitats where DA was potentially produced and accumulated: coastal-pelagic regions). It also allowed me to identify the primary route of toxin transfer during summer 2018: via newly produced blooms in the euphotic zone and the direct accumulation of DA by anchovies.

Isotope results from krill suggest an important link between elemental cycling, coastal productivity, and DA accumulation. The $\delta^{13}C$ in primary consumers like krill

should be used systematically to evaluate spatial differences in elemental cycling that might be linked to sites of *Pseudo-nitzschia* blooms and DA events in non-coastal zones. Additionally, the variation in baseline $\delta^{15}N$ values among habitats in Monterey Bay can be used to identify the habitat of resident consumers that have accumulated high levels of DA, thus providing evidence of regions affected by DA. By knowing when a given habitat has been impacted by DA at a given point in time, fishery closures can be more targeted, which will reduce economic hardships to local communities.

My study highlights subtle but important differences in anchovy foraging strategies that make them more suitable indicators of DA presence in coastal-pelagic regions than other forage species like market squid, juvenile rockfish, and krill, and true specialists like mussels. Anchovies occupy critical intermediate trophic positions, are important prey for a variety of predators, and transfer energy and biomass to higher trophic levels in upwelling systems such as the CCS (Ryther, 1969; Rykaczewski and Checkley, 2008; Szoboszlai et al., 2015). As they are fairly mobile schooling fish and potential prey of many piscivorous predators, anchovies may rapidly disperse DA throughout the food web (Madigan et al., 2012; Szoboszlai et al., 2015; Koehn et al., 2016). In conclusion, I strongly recommend incorporating DA measurements from anchovies into routine sampling protocols to monitor for DA presence and accumulation in coastal-pelagic regions because of their potential to serve as DA vectors, and as complementary indicator species to mussels.

FUTURE WORK

Results from my study offer suitable grounds to support future work. For future research on food web structure, collections should consider obtaining phytoplankton samples from sites where isotope values from other consumers were analyzed. The exact species composition of phytoplankton at sites where krill were collected (at least from this study) would offer more detailed information on the drivers of spatial differences in $\delta^{13}C$ in Monterey Bay, which is necessary to understand community structure. It may also be useful to incorporate compound specific isotope analysis from source amino acids for more detailed information on primary producers and their photosynthetic processes, and trophic amino acids for more accurate depictions trophic interactions.

Future research should also focus more broadly on sea lions and their capacity to serve as sentinel species for DA events. By collecting multiple tissues from stranded sea lions with suspected DA toxicosis for isotope analysis and integrating such data with DA measurements, it may be possible to identify where exactly sea lions are ingesting high levels of toxins. A detailed diet study that incorporates more potential prey items of sea lions and isotope mixing models may also be useful in determining their susceptibility to DA toxicosis and capacity to serve as sentinel species for DA events.

REFERENCES

Altabet, M.A., Pilskaln, C., Thunell, R., Pride, C., Sigman, D., Chavez, F., Francois, R., 1999. The nitrogen isotope biogeochemistry of sinking particles from the margin of the eastern North Pacific. Deep. Res. Part I Oceanogr. Res. Pap. 46, 655–679.

Anderson, C.R., Berdalet, E., Kudela, R.M., Cusack, C.K., Silke, J., O'Rourke, E., Dugan, D., McCammon, M., Newton, J.A., Moore, S.K., Paige, K., Ruberg, S., Morrison, J.R., Kirkpatrick, B., Hubbard, K., Morell, J., 2019. Scaling up from regional case studies to a global harmful algal bloom observing system. Front. Mar. Sci. 6.

Anderson, C.R., Kudela, R.M., Kahru, M., Chao, Y., Rosenfeld, L.K., Bahr, F.L., Anderson, D.M., Norris, T.A., 2016. Initial skill assessment of the California harmful algae risk mapping (C-HARM) system. Harmful Algae 59, 1–18.

Antonelis, G.A., Fiscus, C.H., 1980. The pinnipeds of the California current, California Cooperative Oceanic Fisheries Investigations Report.

Bargu, S., Goldstein, T., Roberts, K., Li, C., Gulland, F.M.D., 2012. *Pseudo-nitzschia* blooms, domoic acid, and related California sea lion strandings in Monterey Bay, California. Mar. Mammal Sci. 28, 237–253.

Bargu, S., Powell, C.L., Coale, S.L., Busman, M., Doucette, G.J., Silver, M.W., 2002. Krill: a potential vector for domoic acid in marine food webs. Mar. Ecol. Prog. Ser. 237, 209–216.

Bargu, S., Powell, C.L., Wang, Z., Doucette, G.J., Silver, M.W., 2008. Note on the occurrence of *Pseudo-nitzschia australis* and domoic acid in squid from Monterey Bay, CA (USA). Harmful Algae 7, 45–51.

Bates, S.S., Bird, C.J., de Freitas, A.S.W., Foxall, R., Giligan, M., Hanic, L.A., Johnson, G.R., McCulloch, A.W., Odense, P., Pocklington, R., Quilliam, M.A., Sim, P.G., Smith, J.C., Subba Rao, D.V., Todd, E.C.., Walter, J.A., Wright, J.L.., 1989. Pennate diatom *Nitzschia pungens* as the primary source of domoic acid, a toxin in shellfish from eastern Prince Edward Island, Canada. Can. J. Fish. Aquat. Sci. 46.

Bates, S.S., Hubbard, K.A., Lundholm, N., Montresor, M., Leaw, C.P., 2018. *Pseudo-nitzschia*, *Nitzschia*, and domoic acid: new research since 2011. Harmful Algae 79, 3–43.

Bowers, H.A., Ryan, J.P., Hayashi, K., Woods, A.L., Marin, R., Smith, G.J., Hubbard, K.A., Doucette, G.J., Mikulski, C.M., Gellene, A.G., Zhang, Y., Kudela, R.M., Caron, D.A., Birch, J.M., Scholin, C.A., 2018. Diversity and toxicity of *Pseudo-nitzschia* species in Monterey Bay: perspectives from targeted and adaptive sampling. Harmful Algae 78, 129–141.

Breaker, L., Broenkow, W.W., 1989. The circulation of Monterey Bay and related processes. Moss Landing Marine Laboratories.

Brinton, E., 1962. The Distribution of Pacific Euphausiids.UC San Diego Bulletin of the Scripps Institute of Oceanography.

Burton, R.K., Koch, P.L., 1999. Isotopic tracking of foraging and long-distance migration in northeastern Pacific pinnipeds. Oecologia 119, 578–585.

California Ocean Science Trust, 2016. Frequently asked questions: Harmful algal blooms and California fisheries.

Checkley, D.M., Barth, J.A., 2009. Patterns and processes in the California Current System. Prog. Oceanogr. 83, 49–64.

Cimino, M.A., Santora, J.A., Schroeder, I., Sydeman, W., Jacox, M.G., Hazen, E.L., Bograd, S.J., 2020. Essential krill species habitat resolved by seasonal upwelling and ocean circulation models within the large marine ecosystem of the California Current System. Ecography (Cop.). 43, 1536–1549.

Costa, D.P., Kuhn, C.E., Weise, M.J., 2007. Foraging ecology of the California sea lion: diet, diving behavior, foraging location, and predation impacts on fisheries resources. California Sea Grant Final Report. 787-798.

Cury, P., Bakun, A., Crawford, R.J.M., Jarre, A., Quiñones, R.A., Shannon, L.J., Verheye, H.M., 2000. Small pelagics in upwelling systems: patterns of interaction and structural changes in "wasp-waist" ecosystems. ICES J. Mar. Sci. 57, 603–618.

DeNiro, M.J., Epstein, S., 1981. Influence of diet on the distribution of nitrogen isotopes in animals. Geochim. Cosmochim. Acta 45, 341–351.

DeNiro, M.J., Epstein, S., 1978. Influence of diet on the distribution of carbon isotopes in animals. Geochim. Cosmochim. Acta 42, 495–506.

Espinoza, P., Bertrand, A., 2008. Revisiting Peruvian anchovy (*Engraulis ringens*) trophodynamics provides a new vision of the Humboldt Current System. Prog. Oceanogr. 37, 215–227.

Flaherty, E.A., Ben-David, M., 2010. Overlap and partitioning of the ecological and isotopic niches. Oikos 119, 1409–1416.

Fox, D.L., Coe, W.R., 1943. Biology of the California sea-mussel (*Mytilus californianus*). J. Exp. Zool. 87, 59–72.

Fritz, L., Quilliam, M.A., Wright, J.L.C., Beale, A.M., Work, T.M., 1992. An outbreak of domoic acid poisoning attributed to the pennate diatom *Pseudonitzschia-australis*. J. Phycol. 28, 439–442.

Frolov, S.A., Kudela, R.M., Bellingham, J.G., 2013. Monitoring of harmful algal blooms in the era of diminishing resources: a case study of the U.S. west coast. Harmful Algae 21–22, 1–12.

Garrison, D.L., 1979. Monterey Bay phytoplankton I. Seasonal cycles of phytoplankton

assemblages. J. Plankton Res. 1, 241–266.

Goericke, R., Fry, B., 1994. Variations in marine plankton $\delta^{13}C$ with latitude, temperature, and dissolved CO_2 in the world ocean. Global Biogeochem. Cycles 8, 85–90.

Goldstein, T., Mazet, J.A.K., Zabka, T.S., Langlois, G., Colegrove, K.M., Silver, M., Bargu, S., Van Dolah, F., Leighfield, T., Conrad, P.A., Barakos, J., Williams, D.C., Dennison, S., Haulena, M., Gulland, F.M.D., 2008. Novel symptomatology and changing epidemiology of domoic acid toxicosis in California sea lions (*Zalophus californianus*): an increasing risk to marine mammal health. Proc. R. Soc. B Biol. Sci. 275, 267–276.

Gómez-Gutiérrez, J., Peterson, W.T., Miller, C.B., 2005. Cross-shelf life-stage segregation and community structure of the euphausiids off central Oregon (1970-1972). Deep Sea Res. II Top. Stud. Oceanogr. 52, 289–315.

Graham, W.M., Largier, J.L., 1997. Upwelling shadows as nearshore retention sites: the example of northern Monterey Bay. Cont. Shelf Res. 17, 509–532.

Greig, D.J., Gulland, F.M.D., Kreuder, C., 2005. A decade of live California sea lion (*Zalophus californianus*) strandings along the central California Coast: causes and trends, 1991-2000. Aquat. Mamm. 31, 11–22.

Gulland, F.M.D., 2000. Domoic acid toxicity in California sea lions (*Zalophus californianus*) stranded along the central California coast, May-October 1998, NOAA Technical Memorandum NMFS.

Gulland, F.M.D., Haulena, M., Fauquier, D., Langlois, G.W., Lander, M.E., Zabka, T., Duerr, R., 2002. Domoic acid toxicity in Californian sea lions: clinical signs, treatment and survival. Vet. Rec. 150, 475–480.

Hallegraeff, G.M., 1993. A review of harmful algal blooms and their apparent global increase. Phycologia 32, 79–99.

Harvey, C., Garfield, N., Williams, G., Tolimieri, N., Schroeder, I., Andrews, K., Barnas, K., Bjorkstedt, E., Bograd, S., Brodeur, R., Burke, B., Cope, J., Coyne, A., DeWitt, L., Dowell, J., Field, J., Fisher, J., Frey, P., Good, T., Greene, C., Hazen, E., Holland, D., Hunter, M., Jacobson, K., Jacox, M., Juhasz, C., Kaplan, I., Kasperski, S., Lawson, D., Leising, A., Manderson, A., Melin, S., Moore, S., Morgan, C., Muhling, B., Munsch, S., Norman, K., Robertson, R., Rogers-Bennett, L., Sakuma, K., Samhouri, J., Selden, R., Siedlecki, S., Somers, K., Sydeman, W., Thompson, A., Thorson, J., Tommasi, D., Trainer, V., Varney, A., Wells, B., Whitmire, C., Williams, M., Williams, T., Zamon, J., Zeman, S., 2019. Ecosystem status report of the California Current for 2019: A summary of ecosystem indicators compiled by the California Current Integrated Ecosystem Assessment Team (CCIEA), NOAA Technical Memorandum NMFS-NWFSC.

Holland, D.S., Leonard, J., 2020. Is a delay a disaster? economic impacts of the delay of the california dungeness crab fishery due to a harmful algal bloom. Harmful Algae 98.

Horner, R.A., Garrison, D.L., Plumley, F.G., 1997. Harmful algal blooms and red tide problems

on the U.S. west coast. Limnol. Oceanogr. 42, 1076–1088.

Hyslop, E.J., 1980. Stomach contents analysis—a review of methods and their application. J. Fish Biol. 17, 411–429.

Ish, T., Dick, E.J., Switzer, P. V., Mangel, M., 2004. Environment, krill and squid in the Monterey Bay: from fisheries to life histories and back again. Deep Sea Res. II 51, 849–862.

Jackson, A.L., Inger, R., Parnell, A.C., Bearhop, S., 2011. Comparing isotopic niche widths among and within communities: SIBER - stable isotope bayesian ellipses in R. J. Anim. Ecol. 80, 595–602.

Jackson, A.L., Parnell, A.C., 2020. Package 'SIBER.'

Karpov, K.A., Cailliet, G.M., 1979. Prey composition of the market squid, *Loligo opalescens berry*, in relation to depth and location of capture, size of squid, and sex of spawning squid, California Cooperative Oceanic Fisheries Investigations.

Koehn, L.E., Essington, T.E., Marshall, K.N., Kaplan, I.C., Sydeman, W.J., Szoboszlai, A.I., Thayer, J.A., 2016. Developing a high taxonomic resolution food web model to assess the functional role of forage fish in the California Current ecosystem. Ecol. Modell. 335, 87–100.

Kudela, R.M., Frolov, S.A., Anderson, C.R., Bellingham, J.G., 2012. Leveraging ocean observatories to monitor and forecast harmful algal blooms: a case study of the U.S. west coast.

Lane, J.Q., Raimondi, P.T., Kudela, R.M., 2009. Development of a logistic regression model for the prediction of toxigenic *Pseudo-nitzschia* blooms in Monterey Bay, California. Mar. Ecol. Prog. Ser. 383, 37–51.

Layman, C.A., Araujo, M.S., Boucek, R., Hammerschlag-Peyer, C.M., Harrison, E., Jud, Z.R., Matich, P., Rosenblatt, A.E., Vaudo, J.J., Yeager, L.A., Post, D.M., Bearhop, S., 2012. Applying stable isotopes to examine food-web structure: an overview of analytical tools. Biol. Rev. 87, 545–562.

Layman, C.A., Arrington, D.A., Montana, C.G., Post, D.M., 2007. Can stable isotope ratios provide for community-wide measures of trophic structure? Ecology 88, 42–48.

Lecher, A.L., Mackey, K., Kudela, R., Ryan, J., Fisher, A., Murray, J., Paytan, A., 2015. Nutrient loading through submarine groundwater discharge and phytoplankton growth in Monterey Bay, CA. Environ. Sci. Technol. 49, 6665–6673.

Lefebvre, K.A., Bargu, S., Kieckhefer, T., Silver, M.W., 2002a. From sanddabs to blue whales: the pervasiveness of domoic acid. Toxicon 40, 971–977.

Lefebvre, K.A., Powell, C.L., Busman, M., Doucette, G.J., Moeller, P.D.R., Silver, J.B., Miller, P.E., Hughes, M.P., Singaram, S., Silver, M.W., Tjeerdema, R.S., 1999. Detection of domoic acid in northern anchovies and California sea lions associated with an unusual

mortality event. Nat. Toxins 7, 85–92.

Lefebvre, K.A., Silver, M.W., Coale, S.L., Tjeerdema, R.S., 2002b. Domoic acid in planktivorous fish in relation to toxic *Pseudo-nitzschia* cell densities. Mar. Biol. 140, 625–631.

Lefebvre, K.A., Robertson, A. 2010. Domoic acid and human exposure risks: a review. Toxicon 56, 218-230.

Lelong, A., Hégaret, H., Soudant, P., Bates, S.S., 2012. *Pseudo-nitzschia* (Bacillariophyceae) species, domoic acid and amnesic shellfish poisoning: revisiting previous paradigms. Phycologia 52, 168–216.

Lewitus, A.J., Horner, R.A., Caron, D.A., Garcia-Mendoza, E., Hickey, B.M., Hunter, M., Huppert, D.D., Kudela, R.M., Langlois, G.W., Largier, J.L., Lessard, E.J., RaLonde, R., Rensel, J.J.E., Strutton, P.G., Trainer, V.L., Tweddle, J.F., 2012. Harmful algal blooms along the North American west coast region: history, trends, causes, and impacts. Harmful Algae 19, 133–159.

Liu, K., Kaplan, I.R., 1989. The eastern tropical Pacific as a source of ^{15}N-enriched nitrate in seawater off southern California. Limnol. Oceanogr. 34, 820–830.

Madigan, D.J., Carlisle, A.B., Dewar, H., Snodgrass, O.E., Litvin, S.Y., Micheli, F., Block, B.A., 2012. Stable isotope analysis challenges wasp-waist food web assumptions in an upwelling pelagic ecosystem. Sci. Rep. 2, 1–11.

McCabe, R.M., Hickey, B.M., Kudela, R.M., Lefebvre, K.A., Adams, N.G., Bill, B.D., Gulland, F.M.D., Thomson, R.E., Cochlan, W.P., Trainer, V.L., 2016. An unprecedented coastwide toxic algal bloom linked to anomalous ocean conditions. Geophys. Res. Lett. 43, 10,366-10,376.

McConnaughey, T., McRoy, C.P., 1979. Food-web structure and the fractionation of carbon isotopes in the Bering Sea. Mar. Biol. 262, 257–262.

McManus, M.A., Kudela, R.M., Silver, M.W., Steward, G.F., Donaghay, P.L., Sullivan, J.M., 2008. Cryptic blooms: are thin layers the missing connection? *Estuaries and Coasts* 31, 396-401.

Mekebri, A., Blondina, G.J., Crane, D.B., 2009. Method validation of microcystins in water and tissue by enhanced liquid chromatography tandem mass spectrometry. J. Chromatogr. A 1216, 3147–3155.

Miller, T.W., Brodeur, R.D., 2007. Diets of and trophic relationships among dominant marine nekton within the northern California Current ecosystem. Fish. Bull. 105, 548–559.

Minagawa, M., Wada, E., 1984. Stepwise enrichment of ^{15}N along food chains: further evidence and the relation between $\delta^{15}N$ and animal age. Geochim. Cosmochim. Acta 48, 1135–1140.

Montoya, J.P., 2007. Natural abundance of ^{15}N in marine planktonic ecosystems, in: Stable Isotopes in Ecology and Environmental Science. pp. 176–201.

Murry, B.A., Farrell, J.M., Teece, M.A., Smyntek, P.M., 2006. Effect of lipid extraction on the interpretation of fish community trophic relationships determined by stable carbon and nitrogen isotopes. Can. J. Fish. Aquat. Sci. 63, 2167–2172.

Newsome, S.D., Martinez del Rio, C., Bearhop, S., Phillips, D.L., 2007. A niche for isotopic ecology. Front. Ecol. Environ. 5, 429–436.

Newsome, S.D., Tinker, M.T., Monson, D.H., Oftedal, O.T., Ralls, K., Staedler, M.M., Fogel, M.L., Estes, J.A., 2009. Using stable isotopes to investigate individual diet specialization in California sea otters (*Enhydra lutris nereis*). Ecology 90, 961–974.

Novaczek, I., Madhyastha, M.S., Ablett, R.f., Donald, A., Johnson, G., Nijjar, M.S., Sims, D.E., 1992. Depuration of domoic acid from live bluemussels *Mytilus edulis.* Can. J. Fish. Aquat. Sci. 49, 312-318.

Paduan, J. D., Rosenfeld, L.K., Remotely sensed surface currents in Monterey Bay from shore-based HF radar (coastal ocean dynamics application radar). J. Geophys. Res. 101. 20,669-20,686.

Peacock, M.B., Gibble, C.M., Senn, D.B., Cloern, J.E., Kudela, R.M., 2018. Blurred lines: multiple freshwater and marine algal toxins at the land-sea interface of San Francisco Bay, California. Harmful Algae 73, 138–147.

Peterson, B.J., Fry, B., 1987. Stable isotopes in ecosystem studies. Annu. Rev. Ecol. Evol. Syst. 18, 293–320.

Pinnegar, J.K., Polunin, N.V.C., 1999. Differential fractionation of $\delta^{13}C$ and $\delta^{15}N$ among fish tissues: implications for the study of trophic interactions. Funct. Ecol. 13, 225–231.

Post, D.M., 2002. Using stable isotopes to estimate trophic position: models, methods, and assumptions. Ecology 83, 703–718.

Rau, G.H., Sweeney, R.E., Kaplan, I.R., 1982. Plankton ^{13}C:^{12}C ratio changes with latitude differences between northern and southern oceans. Deep Sea Res. 29, 1035–1039.

Rau, G.H., Chavez, F.P., Friederich, G.E., 2001. Plankton $^{12}C/^{12}C$ variations in Monterey Bay, California: evidence of non-diffusive inorganic carbon uptake b y phytoplankton in an upwelling environment. Deep Sea Res. II 48, 79–94

Reilly, C.A., Echeverria, T.W., Ralston, S., 1992. Interannual variation and overlap in the diets of pelagic juvenile rockfish (Genus: *Sebastes*) off central California. Fish. Bull. 90, 505–515.

Ritzman, J., Brodbeck, A., Brostrom, S., Mcgrew, S., Dreyer, S., Klinger, T., Moore, S.K., 2018. Economic and sociocultural impacts of fisheries closures in two fishing- dependent communities following the massive 2015 U.S. West Coast harmful algal bloom. Harmful Algae 80, 35–45.

Rosenfeld, L.K., Schwing, F.B., Garfield, N., Tracy, D.E., 1994. Bifurcated flow from an upwelling center: a cold water source for Monterey Bay. Cont. Shelf Res. 14, 931–964.

Ruiz-Cooley, R.I., Engelhaupt, D.T., Ortega-Ortiz, J.G., 2012. Contrasting C and N isotope ratios from sperm whale skin and squid between the Gulf of Mexico and Gulf of California: Effect of habitat. Mar. Biol. 159, 151–164.

Ruiz-Cooley, R.I., Gerrodette, T., 2012. Tracking large-scale latitudinal patterns of $\delta^{13}C$ and $\delta^{15}N$ along the E Pacific using epi-mesopelagic squid as indicators. Ecosphere 3.

Ryan, J.P., Chavez, F.P., Bellingham, J.G., 2005. Physical-biological coupling in Monterey Bay, California: topographic influences on phytoplankton ecology. Mar. Ecol. Prog. Ser. 287, 23–32.

Ryan, J.P., Greenfield, D., Marin, R., Preston, C., Roman, B., Jensen, S., Pargett, D., Birch, J.M., Mikulski, C.M., Doucette, G.J., Scholin, C.A., 2011. Harmful phytoplankton ecology studies using an autonomous molecular analytical and ocean observing network. Limnol. Oceanogr. 56, 1255–1272.

Ryan, J.P., Kudela, R.M., Birch, J.M., Blum, M., Bowers, H.A., Chavez, F.P., Doucette, G.J., Hayashi, K., Marin, R., Mikulski, C.M., Pennington, J.T., Scholin, C.A., Smith, G.J., Woods, A.L., Zhang, Y., 2017. Causality of an extreme harmful algal bloom in Monterey Bay, California, during the 2014-2016 northeast Pacific warm anomaly. Geophys. Res. Lett. 44, 5571–5579.

Ryan, J.P., McManus, M.A., Kudela, R.M., Artigas, M.L., Bellingham, J.G., Chavez, F.P., Doucette, G.J., Foley, D.G., Godin, M.A., Harvey, J.T., Marin, R., Messie, M., Mikulski, C.M., Pennington, T.J., Py, F., Rajan, K., Shulman, I., Wang, Z., Zhang, Y., 2014. Boundary influences on HAB phytoplankton ecology in a stratification-enhanced upwelling shadow. Deep Sea Res. II 101, 63–79.

Rykaczewski, R.R., Checkley, D.M., 2008. Influence of ocean winds on the pelagic ecosystem in upwelling regions. Proc. Natl. Acad. Sci. U.S.A. 105, 1965–1970.

Ryther, J.H., 1969. Photosynthesis and fish production in the sea. Science (80-.). 166, 72–76.

Santora, J.A., Field J.C., Schroder, I.D., Sakuma, K.M., Wells, B.K., Sydeman, W.J. 2012. Spatial ecology of krill, micronekton and top predators in the central California Current: Implications for defining ecologically important areas. Prog. Oceanogr. 106, 154–174.

Saino, T., Hattori, A., 1980. ^{15}N natural abundance in oceanic suspended particulate matter. Nature 283, 752–754.

Scholin, C.A., Gulland, F.M.D., Doucette, G.J., Benson, S., Busman, M., Chavez, F.P., Cordaro, J., DeLong, R., De Vogelaere, A., Harvey, J.T., Haulena, M., Lefebvre, K.A., Lipscomb, T., Loscutoff, S., Lowenstine, L., Marin, R., Miller, P.E., McLellan, W.A., Moeller, P.D.R., Powell, C.L., Rowles, T.K., Silvagni, P., Silver, M.W., Spraker, T., Trainer, V.L., Van Dolah, F.M., 2000. Mortality of sea lions along the central California coast linked to a toxic diatom bloom. Lett. to Nat. 403, 80–84.

Sekula-Wood, E., Schnetzer, A., Benitez-Nelson, C.R., Anderson, C.R., Berelson, W.M., Brzezinski, M.A., Burns, J.M., Caron, D.A., Cetinic, I., Ferry, J.L., Fitzpatrick, E., Jones,

B.H., Miller, P.E., Morton, S.L., Schaffner, R.A., Siegel, D.A., Thunell, R., 2009. Rapid downward transport of the neurotoxin domoic acid in coastal waters. Nat. Geosci. 2, 272–275.

Smith, B.N., Epstein, S., 1971. Two categories of $^{13}C/^{12}C$ ratios for higher plants. Plant Physiol. 47, 380–384.

Smith, J., Connell, P., Evans, R.H., Gellene, A.G., Howard, M.D.A., Jones, B.H., Kaveggia, S., Palmer, L., Schnetzer, A., Seegers, B.N., Seubert, E.L., Tatters, A.O., Caron, D.A., 2018. A decade and a half of *Pseudo-nitzschia* spp. and domoic acid along the coast of southern California. Harmful Algae 79, 87–104.

Stevens, B., Armstrong, D., Cusimano, R., Feeding habits of the dungeness crab *Cancer magister* as determined by the index of relative importance. Mar. Biol. 72, 135-145.

Sun, J., Hutchins, D.A., Feng, Y., Seubert, E.L., Caron, D.A., Fu, F.-X., 2011. Effects of changing pCO_2 and phosphate availability on domoic acid production and physiology of the marine harmful bloom diatom *Pseudo-nitzschia* multiseries. Limnol. Oceanogr. 56, 829–840.

Szoboszlai, A.I., Thayer, J.A., Wood, S.A., Sydeman, W.J., Koehn, L.E., 2015. Forage species in predator diets: synthesis of data from the California Current. Ecol. Inform. 29, 45–56.

Thompson, A.R., Schroeder, I.D., Bograd, S.J., Hazen, E.L., Jacox, M.G., Leising, A.W., 2018. State of the California Current 2017-18: Still not quite normal in the north and getting interesting in the south. Cooperative Oceanic Fisheries Investigations Report. 59.

Trainer, V.L., Bates, S.S., Lundholm, N., Thessen, A.E., Cochlan, W.P., Adams, N.G., Trick, C.G., 2012. *Pseudo-nitzschia* physiological ecology, phylogeny, toxicity, monitoring and impacts on ecosystem health. Harmful Algae 14, 271–300. https://doi.org/10.1016/j.hal.2011.10.025

Trainer, V.L., Moore, S.K., Hallegraeff, G.M., Kudela, R.M., Clement, A., Mardones, J.I., Cochlan, W.P., 2020. Pelagic harmful algal blooms and climate change: lessons from nature's experiments with extremes. Harmful Algae 91.

Trainer, V.L., Nicolaus, A.G., Bill, B.D., Stehr, C.M., Wekell, J.C., Moeller, P.D.R., Busman, M., Woodruff, D., 2000. Domoic acid production near California coastal upwelling zones, June 1998. Limnol. Oceanogr. 45, 1818–1833.

Umhau, B.P., Benitez-Nelson, C.R., Anderson, C.R., McCabe, K., Burrell, C., 2018. A time series of water column distributions and sinking particle flux of *Pseudo-Nitzschia* and domoic acid in the Santa Barbara Basin, California. Toxins. 10.

Van Der Lingen, C.D., Bertrand, A., Bode, A., Brodeur, R.D., Cubillos, P.E., Friedland, K., Garrido, S., Irigoien, X., Miller, T.W., Mollmann, C., Rodriguez-Sanchez, R., Tanaka, H., Temming, A., 2009. Trophic dynamics, in: Checkley, D.M., Alheit, J., Oozeki, Y., Roy, C. (Eds.), Climate Change and Small Pelagic Fish. p. 333.

Van Der Lingen, C.D., Hutchings, L., Field, J.G., 2006. Comparative trophodynamics of

anchovy *Engraulis encrasicolus* and sardine *Sardinops sagax* in the southern Benguela: are species alternations between small pelagic fish trophodynamically mediated? African J. Mar. Sci. 28, 465–477.

Vander Zanden, M.J., Clayton, M.K., Moody, E.K., Solomon, C.T., Weidel, B.C., 2015. Stable isotope turnover and half-life in animal tissues: a literature synthesis. PLoS One 10, 1–16.

Vigilant, V.L., Silver, M.W., 2007. Domoic acid in benthic flatfish on the continental shelf of Monterey Bay, California, USA. Mar. Biol. 151, 2053–2062.

Weise, M.J., Harvey, J.T., 2008. Temporal variability in ocean climate and California sea lion diet and biomass consumption: implications for fisheries management. Mar. Ecol. Prog. Ser. 373, 157–172.

Wells, M.L., Trainer, V.L., Smayda, T.J., Karlson, B.S.O., Trick, C.G., Kudela, R.M., Ishikawa, A., Bernard, S., Wulff, A., Anderson, D.M., Cochlan, W.P., 2015. Harmful algal blooms and climate change: learning from the past and present to forecast the future. Harmful Algae 49, 68–93.

Wilkerson F.P., Dugdale, R.C., Kudela, R.M., Chavez, F.P. 2000. Biomass and productivity in Monterey Bay, California: contribution of the large phytoplankton. Deep Sea Res. II 47, 1003-1022.

Wohlgeschaffen, G.D., Mann, K.H., Subba Rao, D. V., Pocklington, R., 1992. Dynamics of the phycotoxin domoic acid: accumulation and excretion in two commercially important bivalves. J. Appl. Phycol. 4, 297–310.

Work, T.M., Barr, B., Beale, A.M., Fritz, L., Michael, A., Wright, J.L.C., Url, S., 1993. Epidemiology of domoic acid poisoning in brown pelicans (*Pelecanus occidentalis*) and brandt's cormorants (*Phalacrocorax penicillatus*) in California. J. Zoo Wildl. Med.

APPENDIX A

A.T1: All species collected for isotope analysis and DA measurements organized by taxonomic group. Coastline indicates specimens collected along the Moss Landing Harbor or Santa Cruz Wharf. RREAS: Rockfish Recruitment and Ecosystem Assessment Survey. WCGB: West Coast Groundfish Bottom Trawl Survey. Isotope sample size (n) refers to the total number of individual isotopes sampled from 2018. Those in parentheses indicate the number of individuals collected from 2019. The sample size (n) for DA measurements refers to the number of combined DA measurements that taken from each species.

Common name (species name)	Isotope (n)	Year	Collection Method	Mean domoic acid measurement	
				n	ppm
Algae (*Ulva* spp., *Mazzaella* spp)	9	2018	Coastline	NA	NA
Crustaceans					
Krill (*E. pacifica and T. spinifera)*	10	2018	RREAS/ WCGB	10	0.165
Prawn (*Sergestidae*)	2	2018	WCGB	2	1.14
Dungeness Crab (*M. magister*)	29	2019	R/V Sheila B		NA
Echinoderm					
Urchin (*A. fragilis*)	1	2018	WCGB	1	0.03
Mollusk					
California Mussel (*M. californianus*)	6	2018	Coastline	5	0.25

Turban Snail (*T. funebralis*)	2	2018	Coastline		NA
Market Squid (*D. opalescens*)	28	2018	RREAS/ WCGB	5	0.19
Octopus (*O. deletron*)	1	2018	WCGB	1	0.04
Teleost Fish					
Anchovy (*E. mordax*)	48 (21)	2018 (2019)	RREAS/ WCGB	13	15.03
Sardine (*S. sagax*)	8 (21)	2018 (2019)	RREAS/ WCGB	2	0.42
Juvenile rockfish	46	2018	RREAS/ WCGB	22	0.19
Shortbelly rockfish (*S. jordani*)	19	2018	RREAS/ WCGB	6	0.06
Halfbanded rockfish (*S. semicinctus*)	14	2018	RREAS/ WCGB	7	0.44
Stripetail rockfish (*S. Saxicola*)	10	2018	RREAS	6	0.11
Chilipepper rockfish (*S. goodei*)	3	2018	WCGB	3	0.066
Combfish (*Z. latipimnus*)	2	2018	WCGB	2	0.85
Black Eel (*L. diapterus*)	1	2018	WCGB	1	0.02
CA Grenadier (*N. stelgidolepis*)	1	2018	WCGB	1	0.13
Flatfish (combined)	9	2018	WCGB		0.035
Curfin sole (flatfish) (*P. decurren*)	3	2018	WCGB	3	0.00
Dover Sole (flatfish) (*M. pacifica*)	3	2018	WCGB	3	0.024

Pacific sanddab (flatfish) (*C. sordidus*)	3	2018	WCGB	3	0.123
Predators					
Sea Lion (*Z. californianus*)	8	2018	UCSC – Stranding Network	8	0.024
Spotted Ratfish (*H. colliei*)	1	2018	WCGB	1	0.12

A.T2: Ecological information and proposed foraging strategies of key taxa. Data were compiled from previous research studies. Feeding behavior was determined based on previous fndings, in addition to horizontal and vertical movement capacity. The foraging strategy was determined by interpreting their isotopic niches.

Species	**Feeding Behavior**	**Horizontal Movement**	**Vertical Movement**	**Foraging Strategy**	**Citation**
Sardines	Size selective generalists	Highly mobile	Relatively high, < anchovies	diet and habitat specialists	(Rykaczewski and Checkley, 2008; Van Der Lingen et al., 2009, 2006)
Anchovies	Size selective generalists	Highly mobile	Medium	diet and habitat specialists	(Rykaczewski and Checkley, 2008; Van Der Lingen et al., 2009, 2006)
Juvenile Rockfish	Opportunistic, size selective generalist	Medium	Medium	Habitat specialist; diet generalist	(Reilly et al., 1992)
Krill	Particulate specialist	Medium	Medium; moves with eddies and currents	Habitat specialist; diet generalist	(Brinton, 1962; Cimino et al., 2020; Gómez-Gutiérrez et al., 2005; Miller and Brodeur, 2007)

Sea Lions	Plastic specialists at an individual level; generalists at a population level	High, coastal (within the continental shelf)	Shallow, < 40 meters average given their placement in the continental shelf	Habitat and diet generalist	(Lowry et al., 1991; Weise and Harvey, 2008)
Mussels	Size selective, movement restricted scavengers	Limited	Limited	Habitat and diet specialist	(Fox and Coe, 1943); (Wohlgeschaffen et al., 1992)
Market Squid	Opportunistic generalist	Coastal, high movement with currents; < mobile than sardines, anchovies, and sea lions	Restricted to eddies and currents	Habitat specialist; diet generalist	(Ish et al., 2004; Karpov and Cailliet, 1979)
Dungeness Crab	Opportunistic generalist	Limited	Medium (between deep-benthic and estuarine habitats)	Habitat specialists; diet generalist	(Stevens et al., 1982)

A.T3: DA concentrations for anchovies per station. * indicates that their toxin concentration is at or near the federal regulatory threshold (20 ppm). Collection sites coincide with Fig. 1.

[DA]	Station number
19.461*	117
1.988	110
6.356	212

30.931*	119
28.504*	114
44.492*	116
49.117*	115
3.113	117
5.073	110
2.643	110
1.181	211
1.716	NA
0.869	NA

A.T4: Isotopic niche metrics for each species displayed in Fig 5a. The standard ellipse area (SEA), corrected for sample size (SEA_c), and mean Bayesian standard ellipse area (SEA_b). The 95% confidence intervals (CI) for mean SEA_b were calculated.

	Anchovy	**Krill**	**Juv. RF**	**Sardine**	**Market Squid**	**Mussel**	**Sea Lion**	**Crab**
SEA	0.57	1.93	1.96	0.71	0.95	0.21	1.23	0.55
SEA_c	0.58	2.17	2.01	0.73	0.99	0.26	1.44	0.57
SEA_b (mean)	0.58	2.17	2.03	0.73	0.99	0.48	1.54	0.57
95% CI Upper Bound	0.72	3.59	2.68	1.00	1.38	0.92	2.74	0.79
95% CI Lower Bound	0.44	0.95	1.48	0.5	0.63	0.15	0.56	0.36

A.T5: Percent overlap for species in the full SIBER analysis. Percentage overlap corresponds to the percent of ellipse overlap in Fig. 5a between specified taxa. It is the proportion of non-overlapping area of two ellipses * 100.

Species 1	**Species 2**	**Percent Overlap**

Anchovy	Juvenile Rockfish	27.34%
Anchovy	Sardine	40.00%
Anchovy	Market Squid	50.17%
Sardine	Juvenile Rockfish	19.59%
Sardine	Market Squid	46.23%
Krill	Juvenile Rockfish	13.80%
Market Squid	Krill	4.19%
Market Squid	Juvenile Rockfish	38.60%

A.T6: Isotopic niche metrics for the site-control analysis displayed in Fig 5c. The convex hull total area (TA), standard ellipse area corrected for sample size (SEA_c), and mean Bayesian standard ellipse area (SEA_b) and their 95% confidence intervals (CI). Data for anchovy and sardine includes results from 2018 and 2019. Refer to Fig. 5c for SIBER plot.

	Anchovies	**Krill**	**Juvenile Rockfish**	**Sardine**	**Squid**	**Crab**
SEA	0.45	1.68	0.67	0.19	0.8	0.55
SEA_c	0.48	2.24	0.8	0.23	0.84	0.57
SEA_b (mean)	0.5	2.13	0.83	0.84	0.23	0.57
95% CI Upper Bound	0.7	4.42	1.51	1.2	0.42	0.78
95% CI Lower Bound	0.26	0.55	0.26	0.51	0.08	0.36

A.T7: Metrics for the proportion of isospace that each of the six potential vectors occupy in comparison to the entire subsampled community. Metrics include the standard ellipse area (SEA), SEA corrected for sample size (SEA_c), and mean Bayesian standard ellipse area (SEA_b), which were calculated in SIBER.

	Anchovy	**Krill**	**Juvenile Rockfish**	**Sardine**	**Market Squid**	**Mussel**
SEA	7.89	26.62	27.05	9.75	13.13	2.9

SEA_c	7.98	29.86	27.58	10.08	13.6	3.6
SEA_b (mean)	7.96	29.7	28.3	10.07	13.5	6.5